IEEE NPSS NUCLEAR & PLASMA SCIENCES SOCIETY

MANCHESTER 1824

Silicon and Pixel Detectors

Cinzia Da Vià
The University of Manchester, UK
Stony Brook Univerity USA

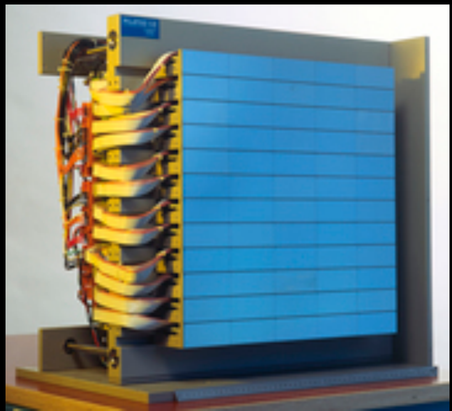

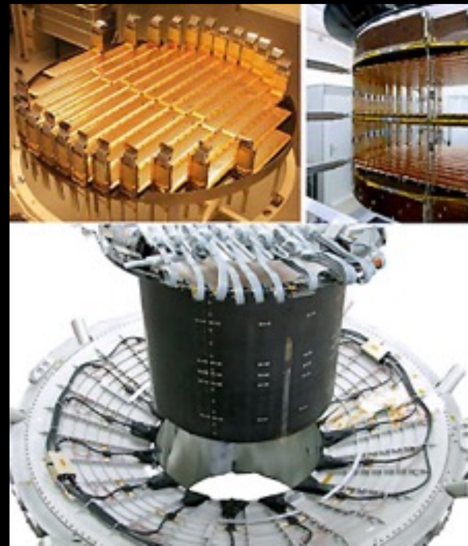

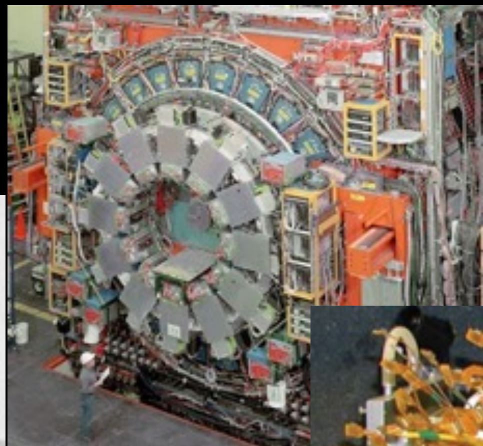

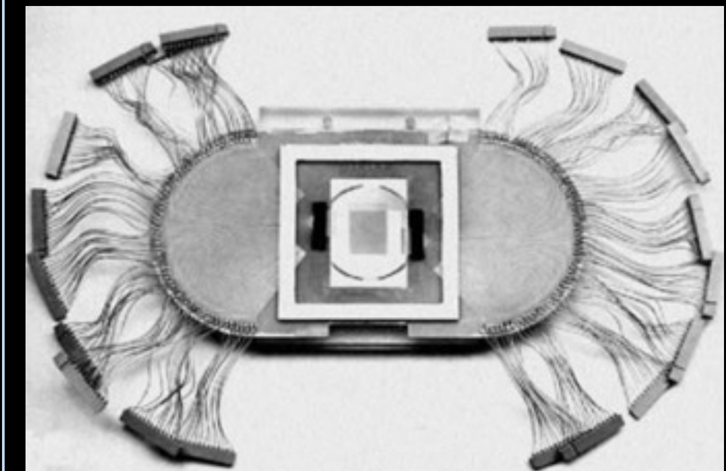

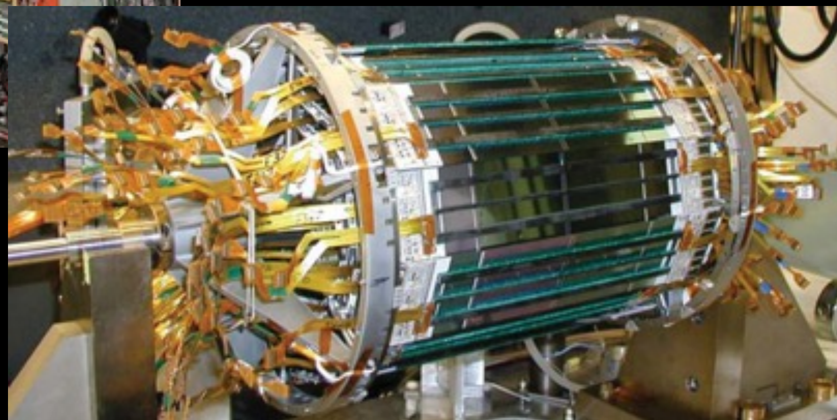

IEEE NPSS Workshop on Applications of Radiation Instrumentation, Dakar 3rd of December 2020

Some Information about myself

- Professor at The University of Manchester (UK)
- Visiting Professor at the University of Stony Brook, New York, USA
- Member of the ATLAS Collaboration at CERN – LHC
- Spent 11 years at CERN during the LHC detector development working on radiation hard pixel detectors

Work Highlights:

- Detector development : scintillating fibers, silicon pixels
- Radiation effects in silicon, low temperature effects (Lazarus)
- 3D sensors for high energy physics and other applications
- 3D printed detectors
- Vertical integrated microsystems
- Quantum Imaging

MANCHESTER 1824

This lecture

- Introduction on Radiation Interaction with Matter
- Why Silicon as a radiation detector
- Silicon radiation detectors: Strip and Pixel sensors Monolithic and Hybrid
- Novel silicon technologies: micro-fabricated 3D sensors, LGADS and microsystems (time permitting)
- Examples of applications in High Energy Physics, Medicine, Environmental Monitoring, Space..

Introduction: Imaging radiation ..

Web cams

Smart phones

photo cameras

machine vision, automotive, security etc…

Medical imaging

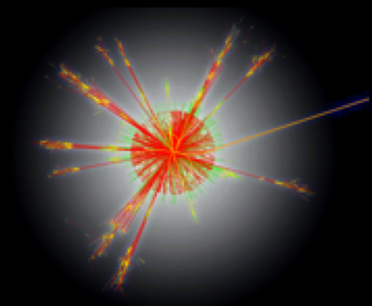

HEP

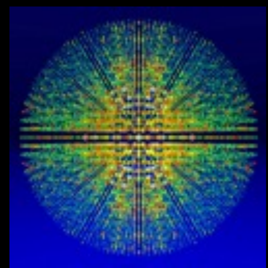

x-ray crystallography

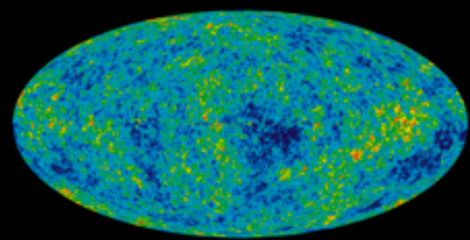

cosmology

mass spectroscopy, neutrons, electrons, TOF, SEM/TEM etc…

MANCHESTER 1824

Reminder: What is Radiation and its interaction with matter

Radiation can be defined as the propagation of energy through space or matter in the form of electromagnetic waves or energetic particles.

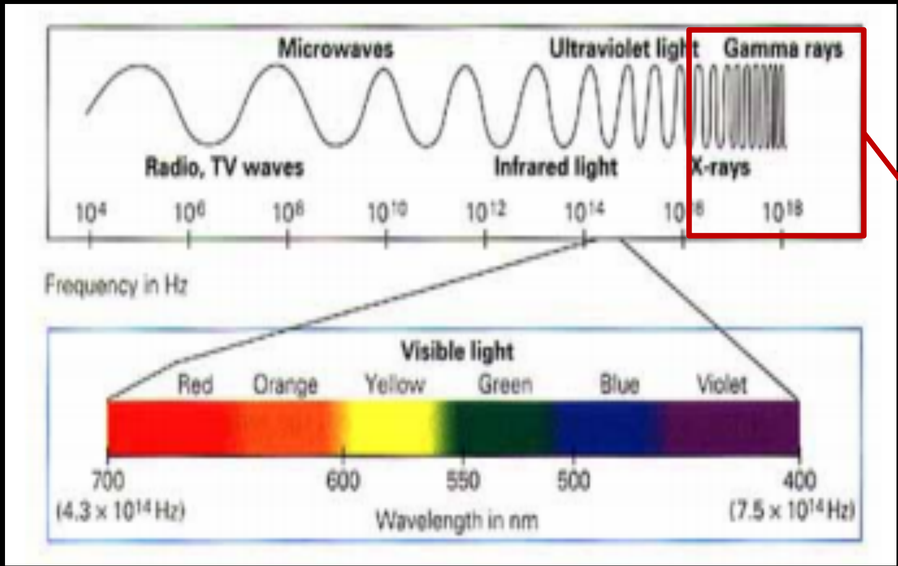

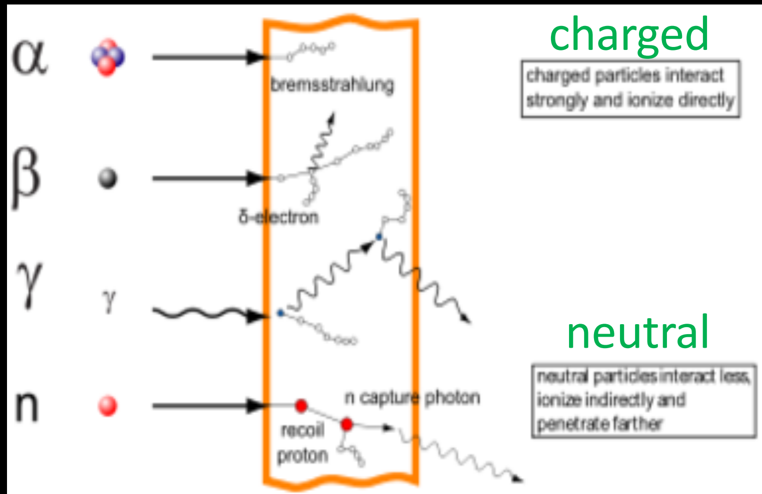

When radiation interacts with matter:

Non-ionizing does not have enough energy to ionize atoms but generate heat in the material it interacts with. At high energy it becomes ionizing

Ionizing has the ability to knock an electron from an atom, i.e. to ionize..

Interaction of radiation with matter

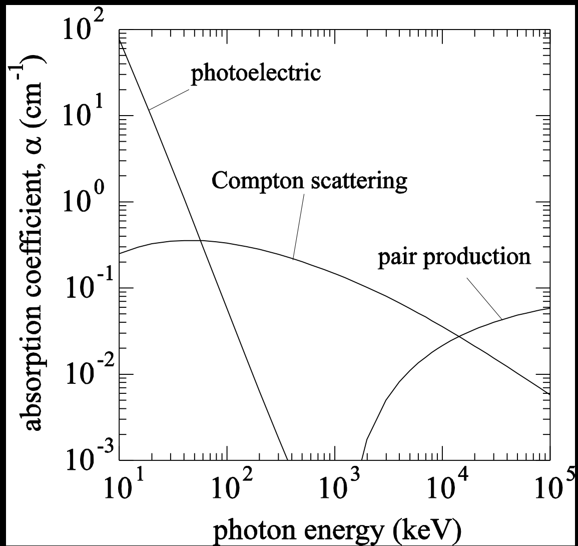

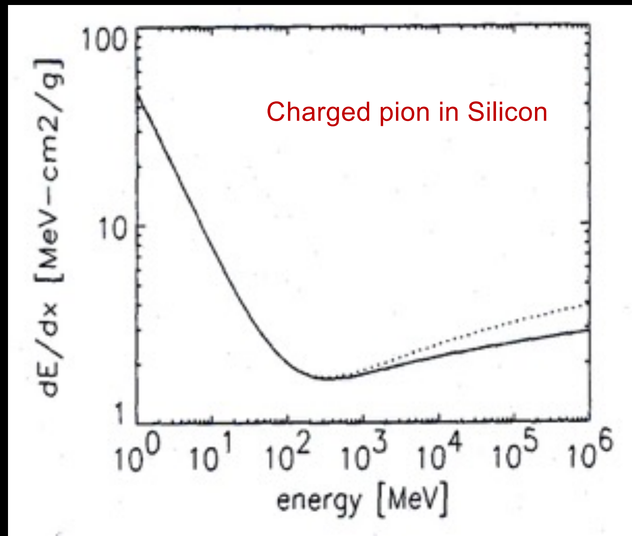

Photons:

There are 3 main modes of interaction:

- -Photoelectric absorption
- -Electron scattering
- -Pair production

Lambert-Beer's law

$$\phi(x) = \phi_0 \cdot e^{-\alpha x}$$

Ionizing particles:

Bethe-Bloch equation:
average/mean amount of energy lost due to ionization per unit of distance in the media)

$$-\frac{dE}{dx} = \frac{4\pi}{m_e c^2} \cdot \frac{n z^2}{\beta^2} \cdot \left(\frac{e^2}{4\pi\varepsilon_0}\right)^2 \cdot \left[\ln\left(\frac{2m_e c^2 \beta^2}{I \cdot (1-\beta^2)}\right) - \beta^2\right]$$

$$n = \frac{N_A \cdot Z \cdot \rho}{A \cdot M_u}$$

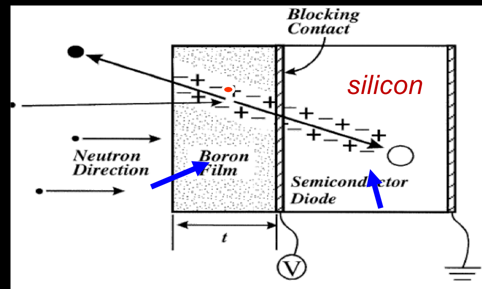

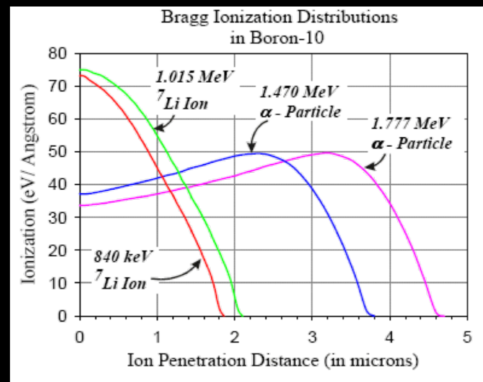

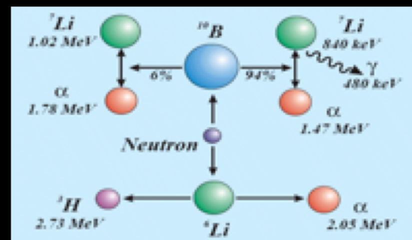

Neutrons: Alpha Bragg peak

Particle signatures with the Timepixel detector

→See next talk on Timepix detectors

5 KeV X-rays | 2MeV electrons | α

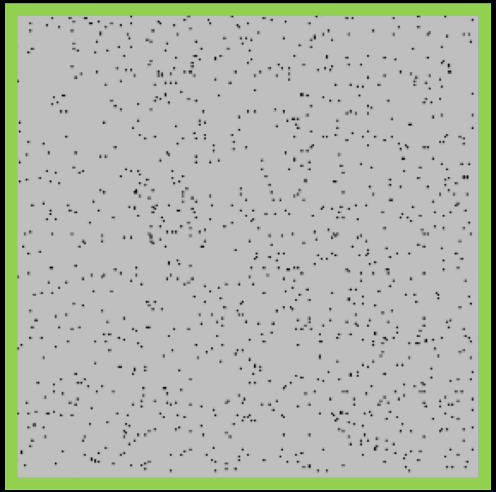

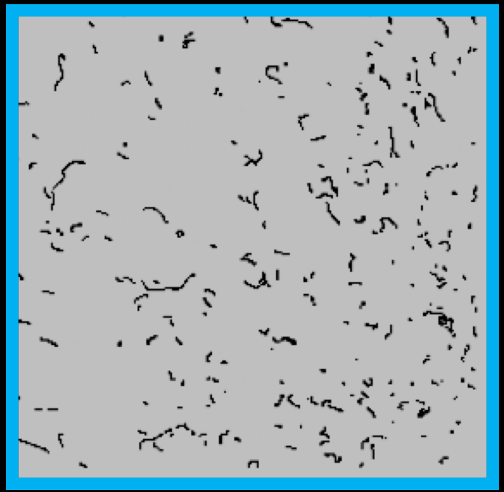

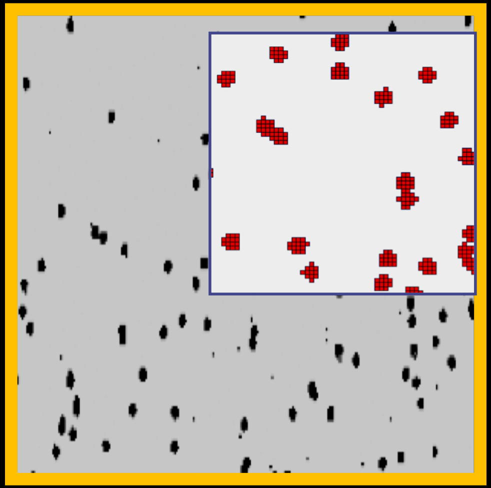

- [241]Am alpha source gives clusters of ~5x5 pixels measured with the MEDIPIX-USB device and a 300 μm thick silicon sensor. The clusters are shown in detail in the inlet. The cluster sizes depend on particle energy and threshold setting.
- Signature of X-rays from a [55]Fe X-ray source. Photons yield single pixel hits or hits on 2 adjacent pixels due to charge sharing.
- A [90]Sr beta source produces curved tracks in the silicon detector.
- A pixel counter is used just to say "YES" if individual quantum of radiation generates in the pixel a charge above the pre-selected threshold

The semiconductors revolution

First transistor invented 1947 by William B. Shockley, John Bardeen and Walter Brattain (Nobel Prize 1956)

First semiconductor particle sensor: Pieter Jacobus Van Heerden, *The Crystalcounter: A New Instrument in Nuclear Physics.* University Math Naturwiss, Fak (1945). *CCD Nobel prize Boyle & Smith 2009*

A **Semiconductor** is a material that has a conductivity between a conductor and an insulator; electricity can pass through it, but not very easily

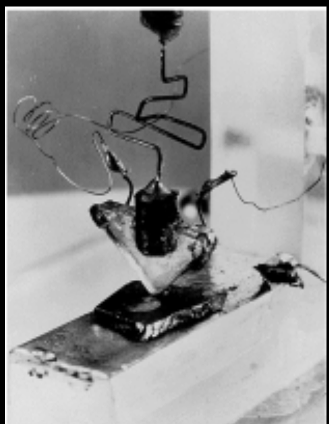

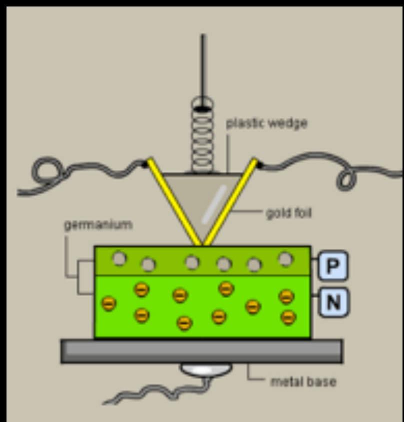

The point contact germanium transistor

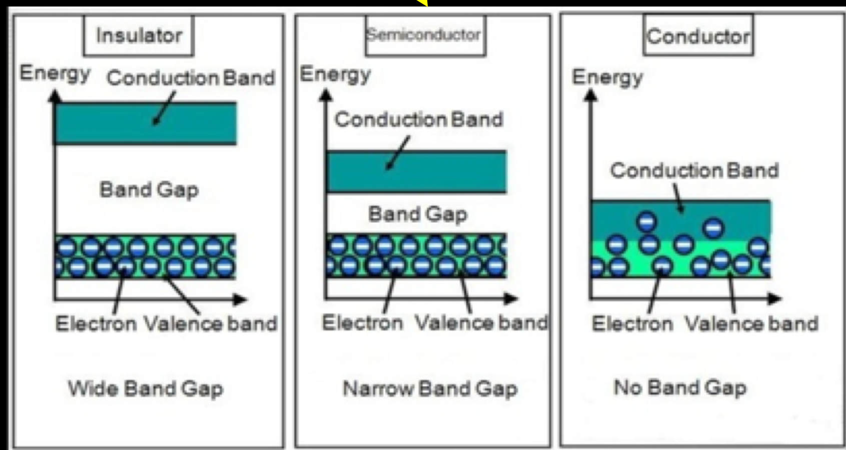

Why Silicon is still the most used

- Semiconductor with Low ionization energy → big signal
  The band gap is 1.12 eV, but it takes 3.6 eV to ionize an atom. The remaining energy goes to phonon excitations (heat)
- **High purity → long carrier lifetime**
- High mobility →fast charge collection
- Low Z→ Z=14 low multiple scattering but low x-ray detection efficiency
- Oxide (SiO_2) has excellent electrical properties
- Good mechanical properties→ Easily patterned to small dimensions
- Can be operated in air and at room temperature (before irradiation –afterwards requires cooling)
- Industrial experience and commercial applications
- **Silicon is abundant! Over 90% of the Earth's crust is composed of <u>silicate minerals</u>**

making silicon the second most abundant element in the Earth's crust (about 28% by mass) after oxygen

Parameter	cBN	hBN	Diamond	AlN	GaN	3C-SiC	GaAs	Si
Energy Bandgap (eV)	6.4	5.2	5.45	6.2	3.39	3.00	1.43	1.12
Electron Mobility (cm^2/Vs)	280	-	2200	300	440	400	8500	1500
Hole Mobility (cm^2/Vs)	-	-	1600	30	~20	50	400	600
Thermal Conductivity (W/cm K)	13	a = 6.0 c = 0.3	20	2.9	1.3	5	0.46	1.5
Breakdown (x 10^5 Vcm^{-1})	~80	~80	100	~80	~80	40	60	3
Lattice Constant (Å)	3.615	a = 2.504 c = 6.661	3.567	4.982	a = 3.189 c = 5.185	4.358	5.65	5.43
Thermal Expansion Coefficient (x 10^{-6} $℃^{-1}$)	3.5	a = -2.7 c = 38	1.1	4.0	4.5	4.7	5.9	2.6
Density (gm/cm^3)	3.487	2.28	3.515	3.26	6.15	3.216	5.316	2.328
Melting Point (℃)	2973	3000	3800	2200	>2500	2540	1238	1420
Dielectric Constant	7.1	5.1	5.5	-	9.5	9.7	12.5	11.8
Resistivity (Ωcm)	10^{16}	10^{10}	10^{13}	10^{14}	10^{12}	150	10^8	10^3
Absorption Edge (μm)	0.205	0.212	0.20	-	0.35	0.40	-	1.40
Refractive Index	2.17	1.80	2.42	2.00	2.33	2.65	3.4	3.5
Hardness (kg/mm^2), T = 300 K Kg/mm^2	5000	100	10,000	2500	1100	3000	600	1000

SILICON: from sand to wafer

a) The sand is cleaned and further purified by chemical processes. It is then melted. Then a tiny concentration of phosphorus (boron) dopant is added to make n (p) type poly-crystalline ingots

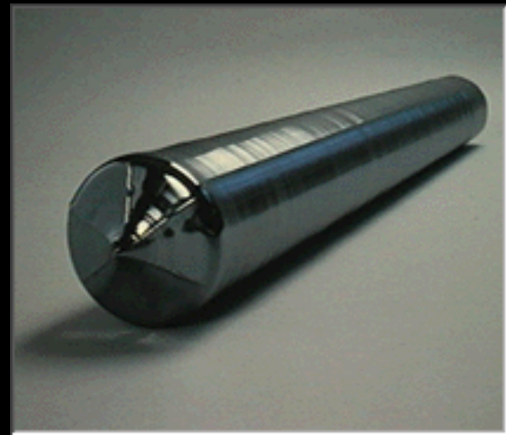

b) Single-crystal silicon is obtained by melting the vertically oriented poly-silicon cylinder onto a single crystal "seed" --- called "Float Zone-→ FZ"

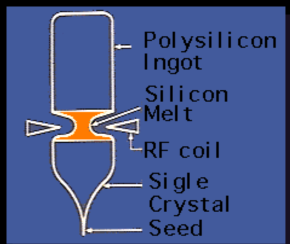

c) Wafers of thickness 200- 500µm are cut with diamond encrusted wire or disc saws.

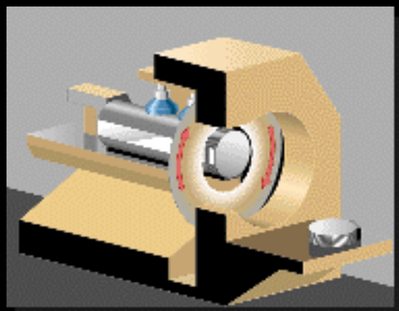

Note: the crystal orientation matters!
<111> and <100> crystals can influence the detector properties eg. capacitance

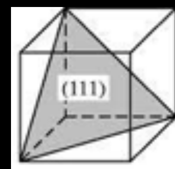

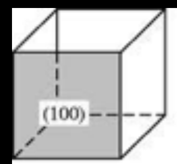

From Wafers to Sensors

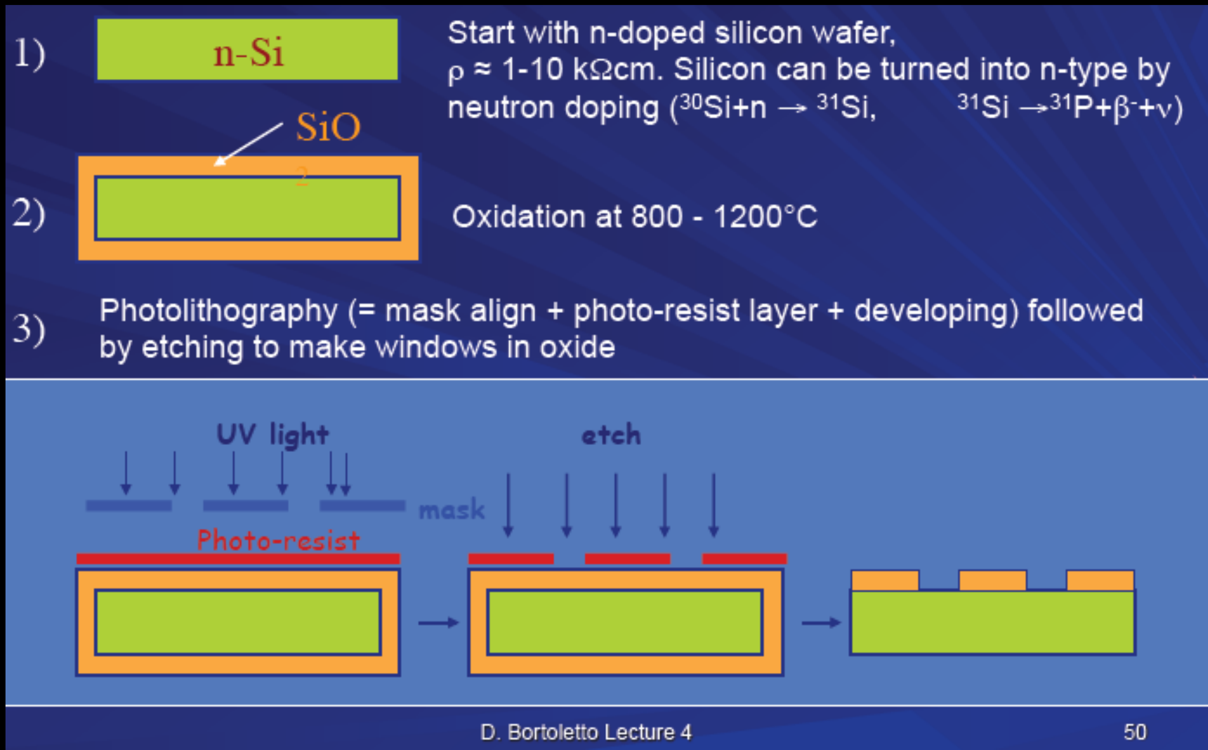

Note:

This process is used for single and double side processing

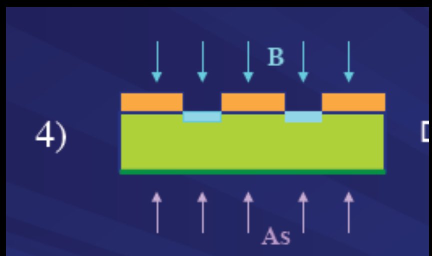

Doping (ion implantation or diffusion)

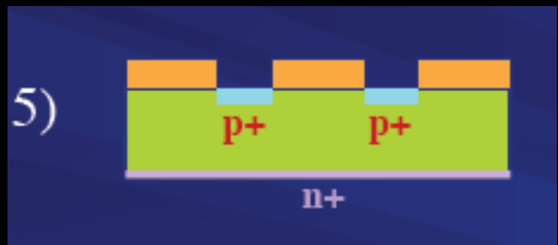

Crystal lattice annealing at 600C

Photo-lithography
Followed by Aluminum
Deposition in the contact
Regions (front and back)

Cinzia Da Via, Uni. Manchester IEEE NPSS Workshop on Applications of Radiation Instrumentation, 2020

Cinzia Da Via, Uni. Manchester IEEE NPSS Workshop on Applications of Radiation Instrumentation, 2020

MANCHESTER 1824

p-n Junction

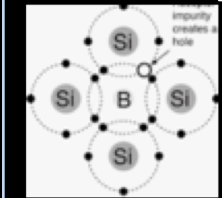

Doping: p-type Silicon

add elements from IIIrd group

⇒ acceptors (B,..)

holes are majority carriers

Doping: n-type Silicon

add elements from Vth group

⇒ donors (P, As,..)

electrons are majority carriers

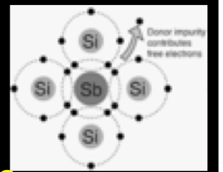

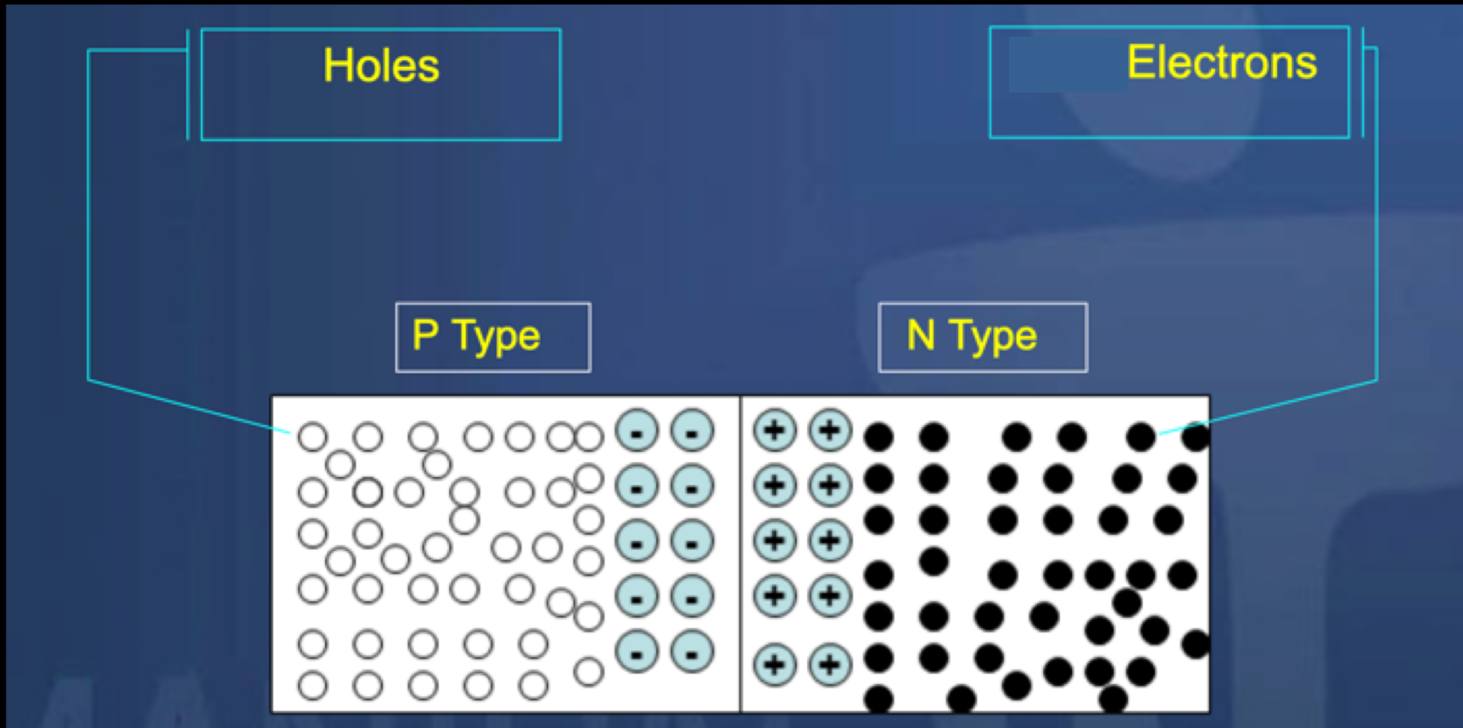

Depletion Region

Silicon detector basic working principle

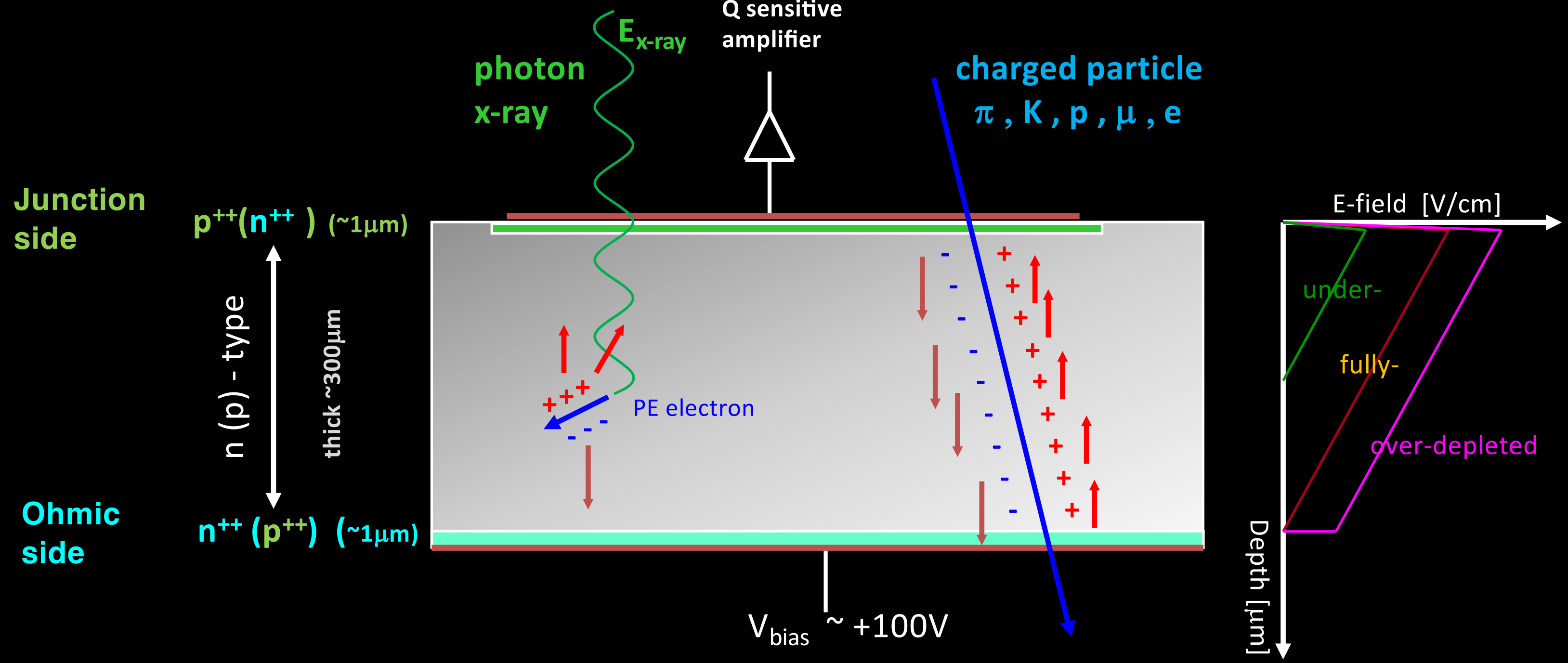

- n+ and p+ electrodes are implanted on the wafer's surfaces to form a p-i-n junction
- V_{bias} is the applied reverse bias voltage, W is the depletion region and Neff the space charge (also called effective doping concentration)
- e-h pairs are created by the energy released by the impinging particle (different interaction mechanism for photons/x-rays and charged particles)
- e-h drift towards the positive and negative electrode "inducing " a current pulse
- Charge collection time depends on the carrier mobility, bias voltage and carrier polarity

$$V_{bias} = \frac{(W)^2 \times e \times |N_{eff}|}{2\varepsilon_0 \varepsilon_{Si}}$$

Segmented Silicon Sensors for better Position Sensitivity

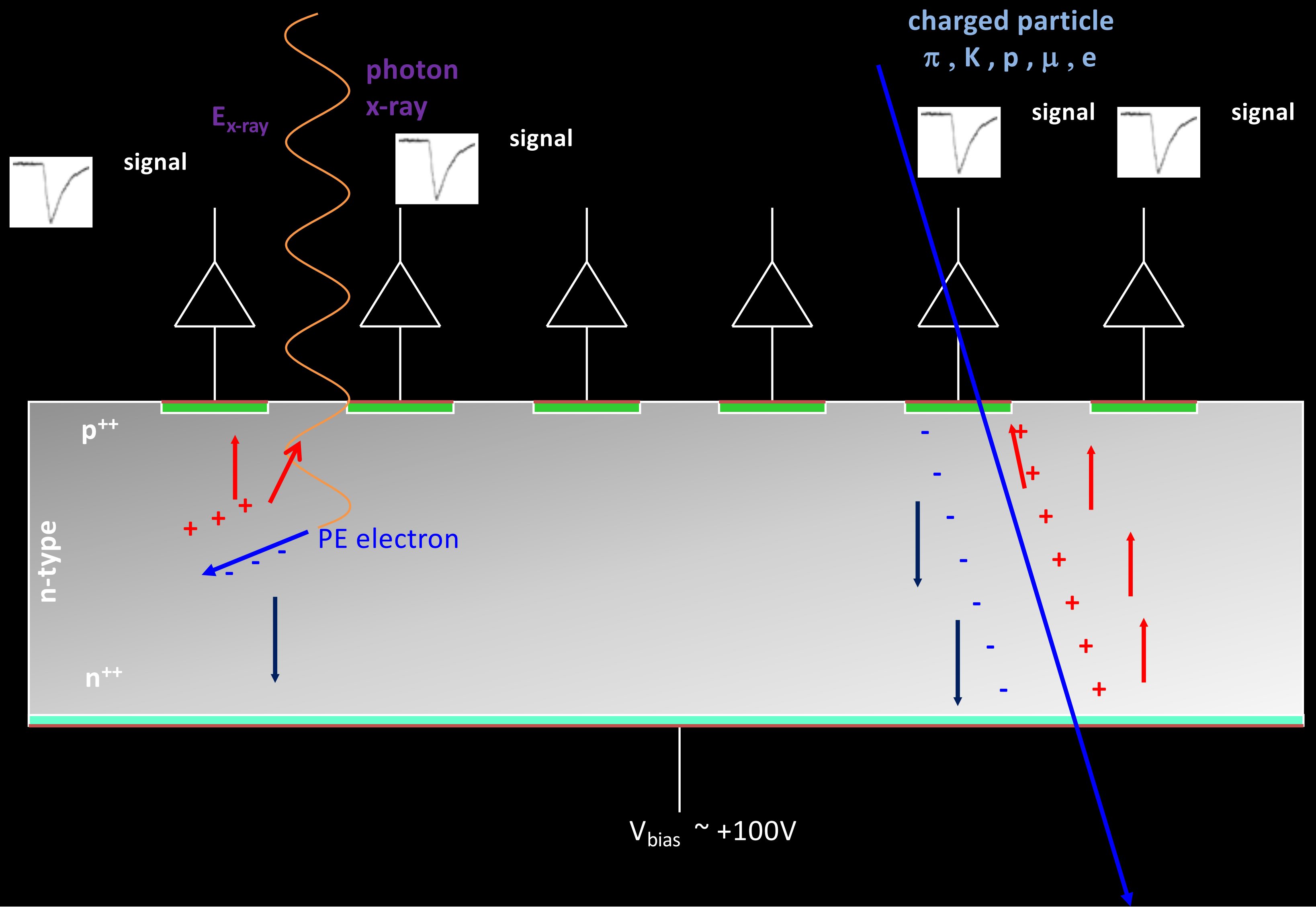

MANCHESTER 1824

Example: CMS micro-strip module

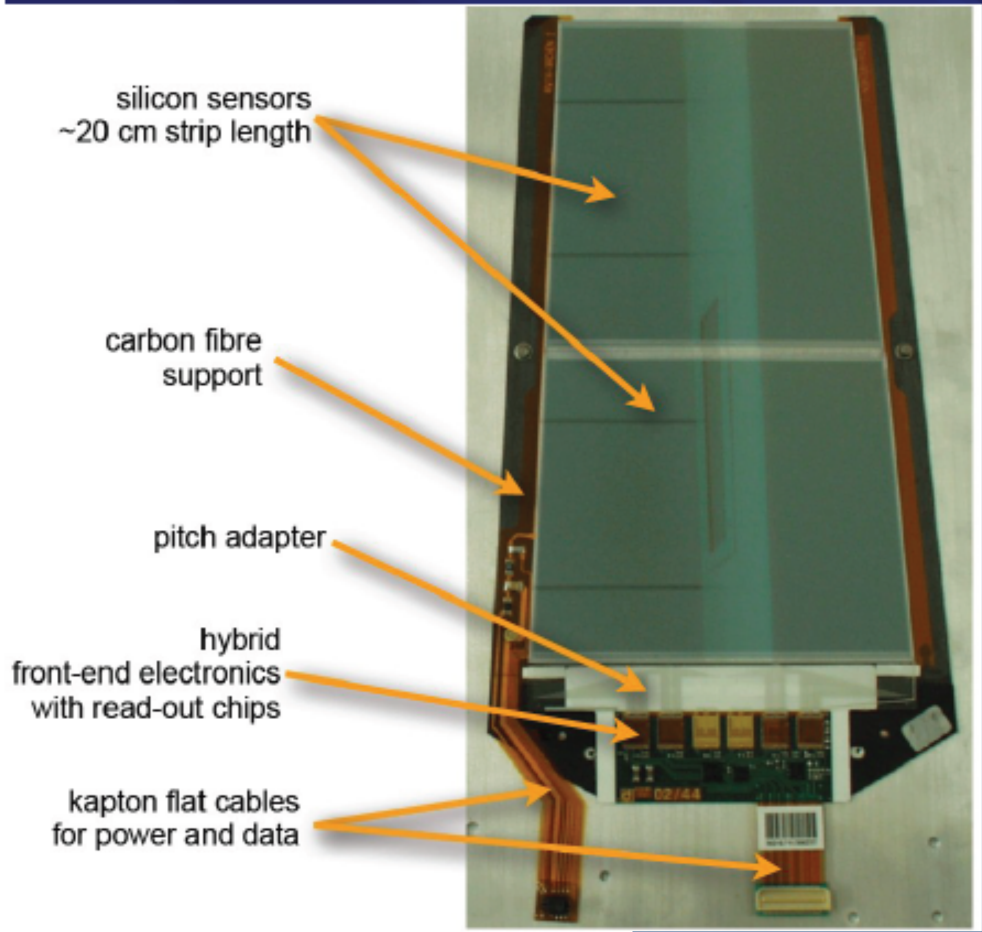

CMS strip module

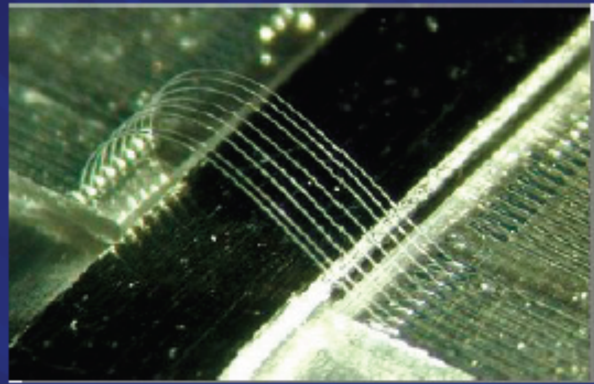

Wire-bonding

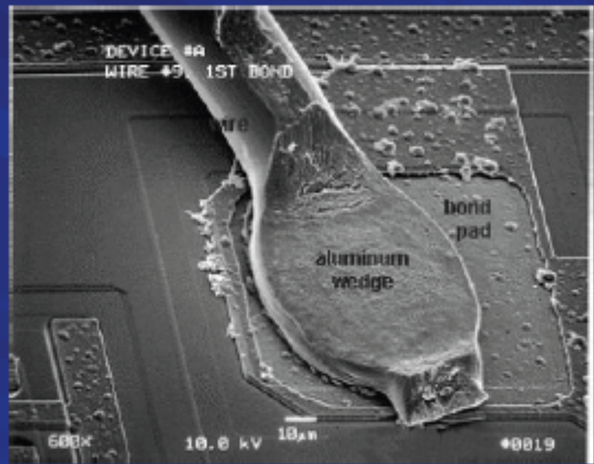

31

Slide from D. Bortoletto

Front-end Readout electronics chain

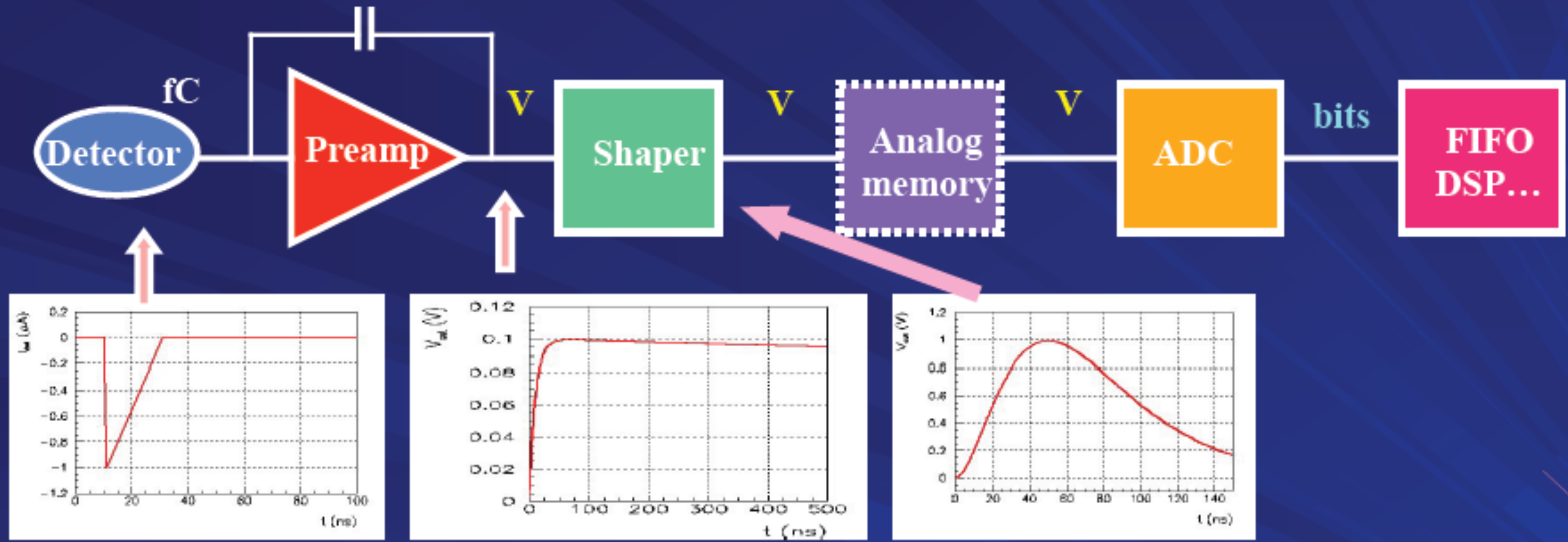

- Very small signals (fC) -> need amplification
- Measurement of amplitude and/or time
  - (ADCs, discris, TDCs) (Example Time over Threshold)
- Several thousands to millions of channels

MANCHESTER 1824

Pixel Detectors "Hybrid"

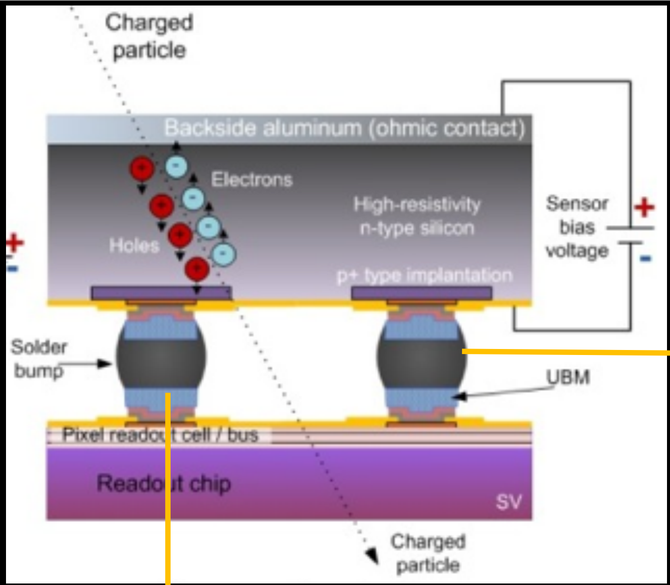

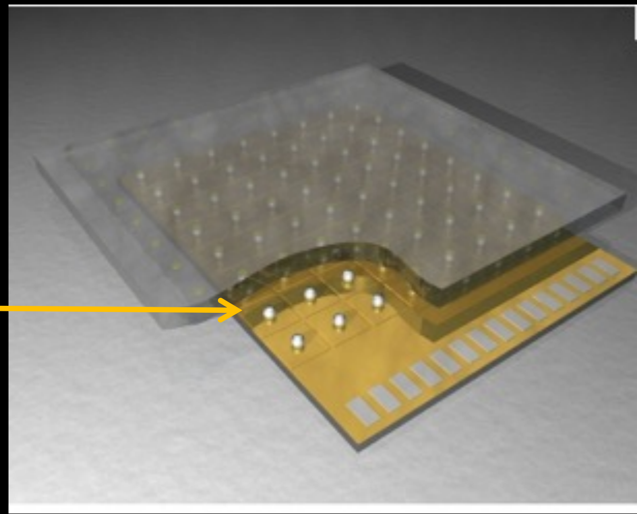

ATLAS FE-I4
80x336
=26 880 pixels
250 x 50 um^2

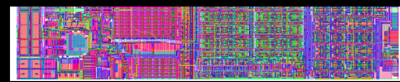

solder

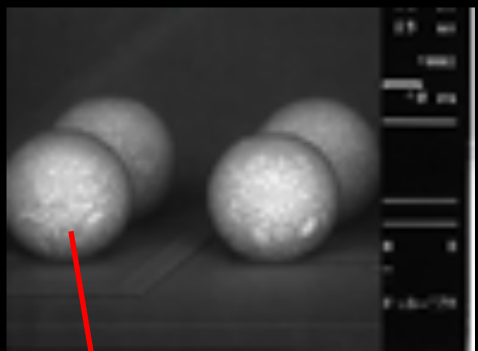

50 microns

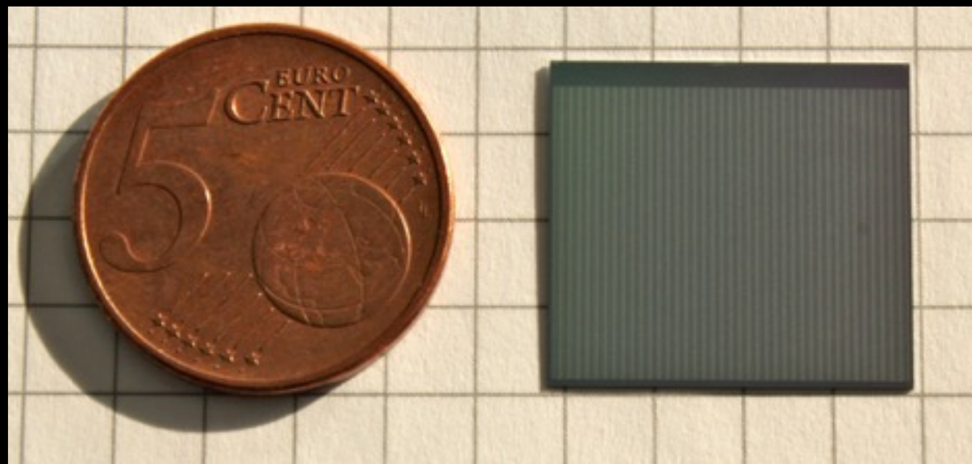

ATLAS FE-I4~4cm^2

Cinzia Da Via, Uni. Manchester IEEE NPSS Workshop on Applications of Radiation Instrumentation, 2020

Example: the ATLAS Pixel "FE-I" Family

	FEI4B	FEI3
Year	2011	2003
Technology	130nm	250nm
Chip size	20x19mm²	7.6x10.8mm²
Active area	89%	74%
Array	80x336 (26'880)	18x160 (2'880)
Pixel size	50x250µm²	50x400µm²
Number of transistors	87M	3.5M
Data rate	320 Mb/s	40Mb/s
Wafer yield	60%	80%

!!

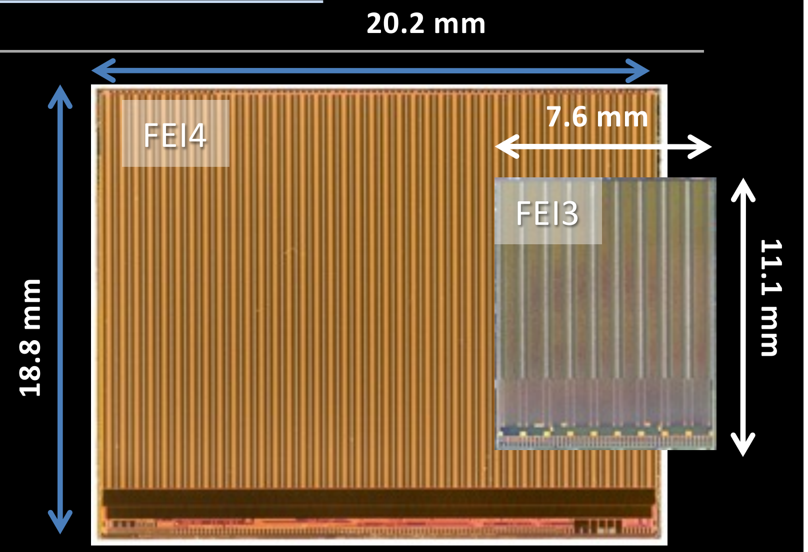

400 µm

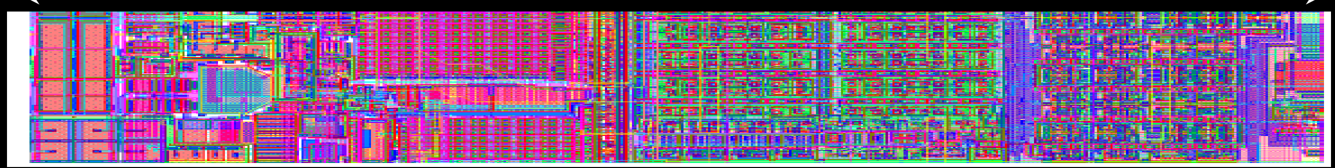

FE-I3 CMOS 250 nm

250 µm FE-I4 CMOS 130 nm

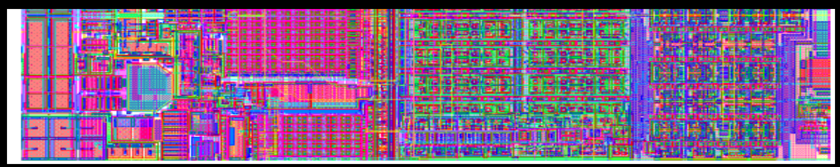

125 µm

FE-I5 CMOS 65 nm

Half pitch definition

Depends on IC designs

250nm-130nm-65nm Technology nodes

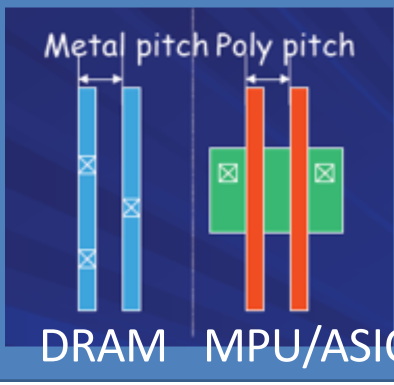

Time Over Threshold Electronics

- 1 TDC (Time to Digital Converter) channel measuring both leading edge and pulse width
- Single threshold timing: as soon as the signal Is above threshold a digital signal is generated

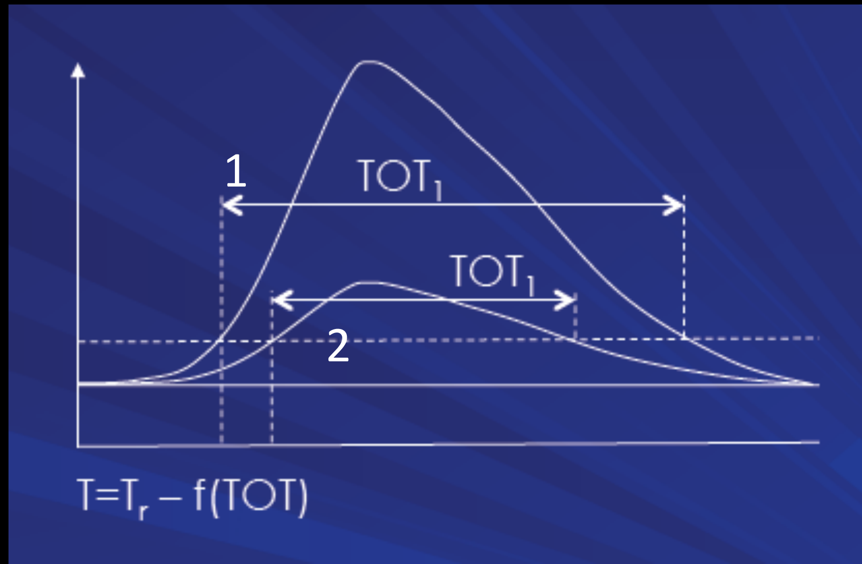

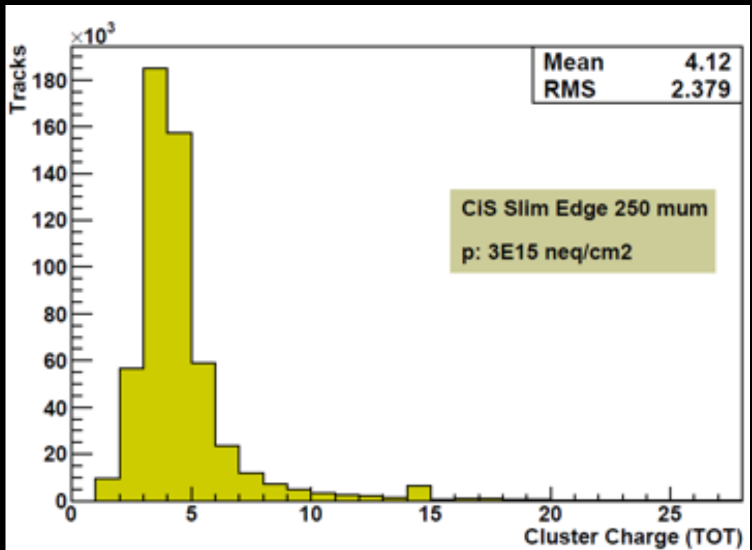

- There is a dependence of the signal rise-time (1 and2) and amplitude ("time walk") which depends on the sensor capacitance C
  - can even be used as an ADC (Analog to Digital Converter)

– E.g. ATLAS Pixel

Pixel detectors “Monolithic”

Integrates the readout circuitry together with the detector in ‘one piece ’ of silicon

The charge generated by a particle is collected on a defined collection electrode either by diffusion or by the application of an E-field

Small pixel size and thin effective detection thickness

Radiation soft, optimal for high granularity applications

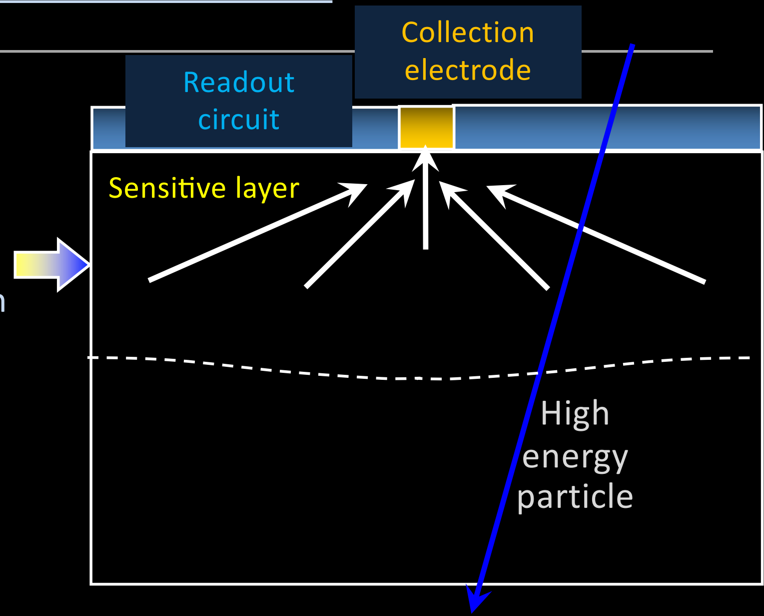

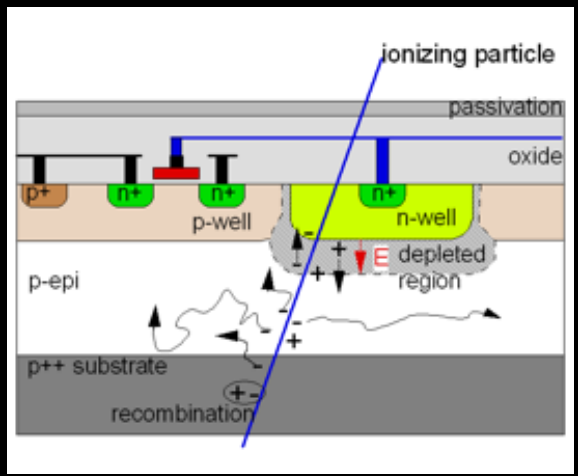

IEEE TNS Vol: 56, Issue: 3, 2009

MAPS

Pixel size :
20 x 20 micron
Thickness
20-50 um

Used in the
EUDET telescope
And at STAR
At RICH

CCD

Charge
coupled
Device
Various
dimensions

Many uses in
Different
fields

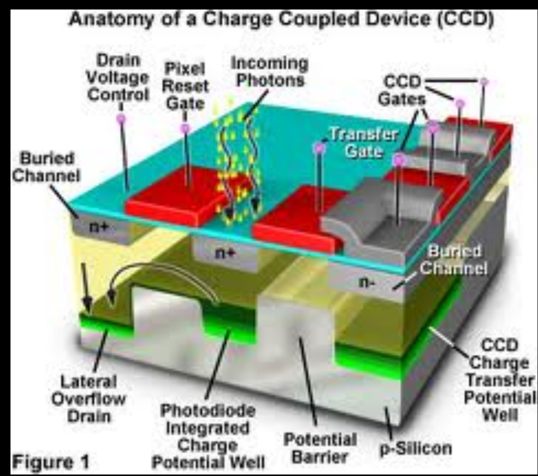

MANCHESTER
1824

Pixels detectors and application requirements

Hybrid

Monolithic

Radiation Hardness

Granularity, low mass

3D sensors

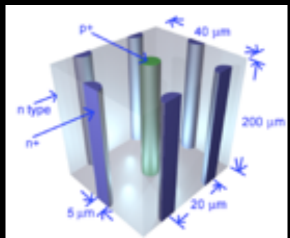

diamond

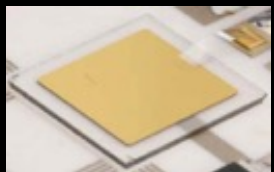

n-in-n, n-in-p-
planar

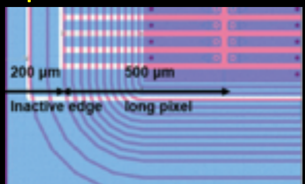

CCD

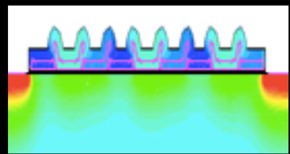

DEPFET

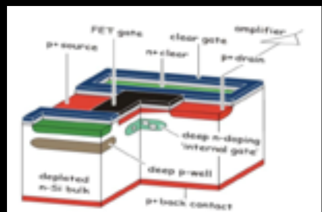

SOI

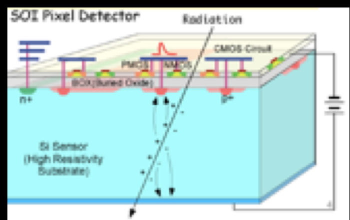

Mimosa

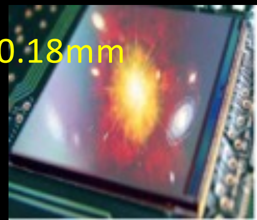

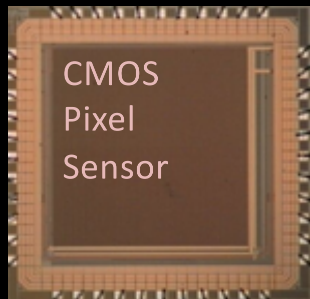

INMAPS

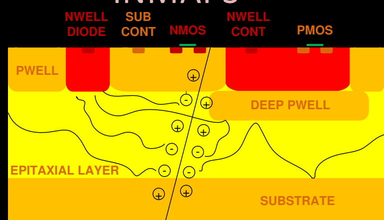

HV-MAPS

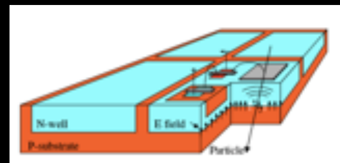

deepNwell

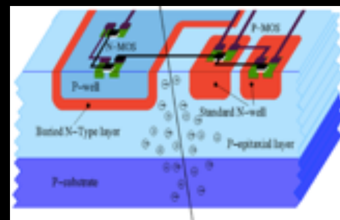

LePiX

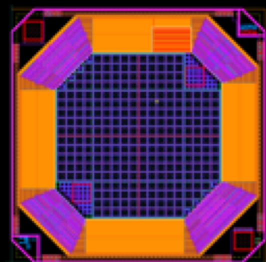

The CERN Large Hadron Collider (LHC)

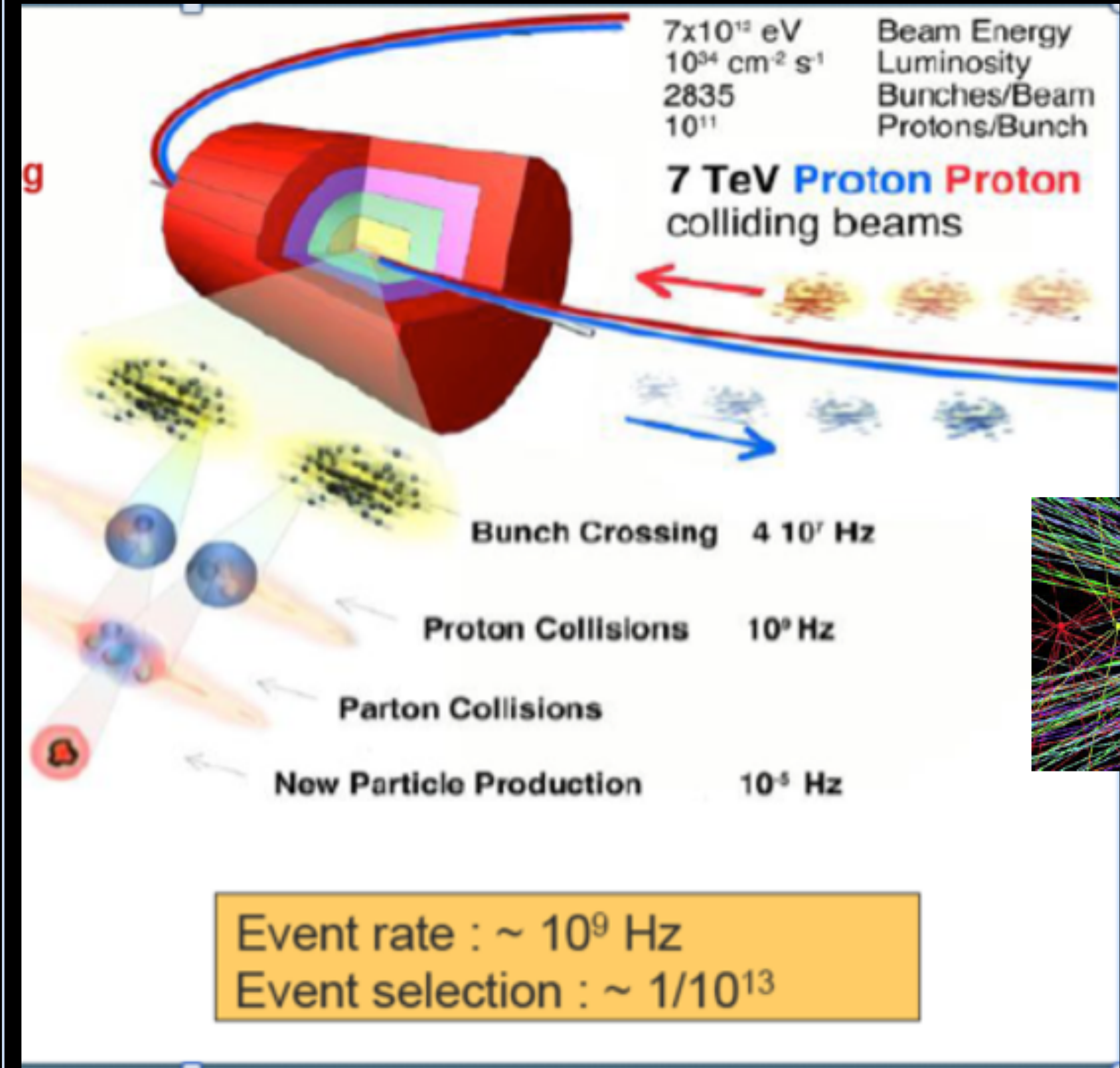

A microscope to observe Dimensions as small as 10^{-17}m!

Collisions every 25 ns

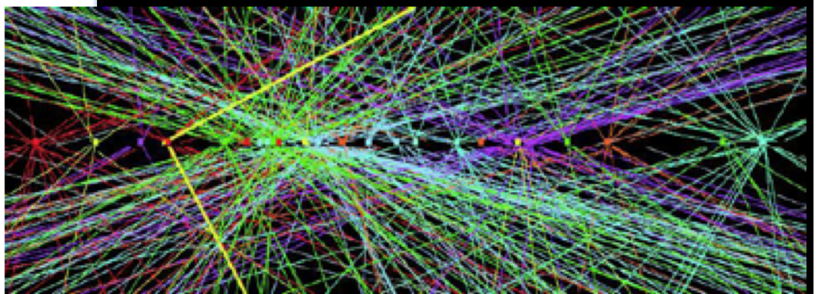

Z -> μμ event at LHC ATLAS 15 April 2012

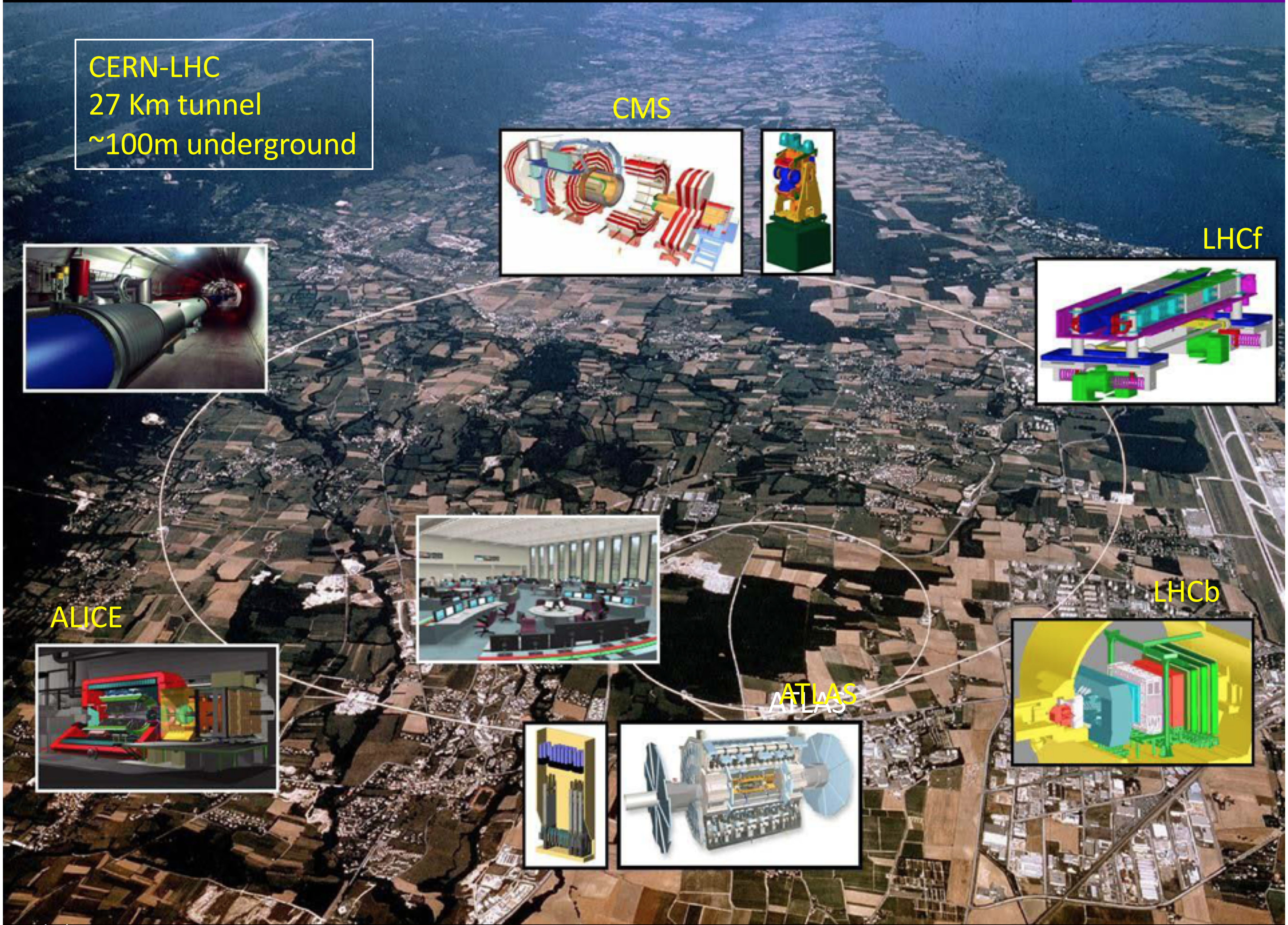
CERN-LHC
27 Km tunnel
~100m underground
CMS
LHCf
ALICE
LHCb
ATLAS

MANCHESTER 1824

A typical particle detector: CMS

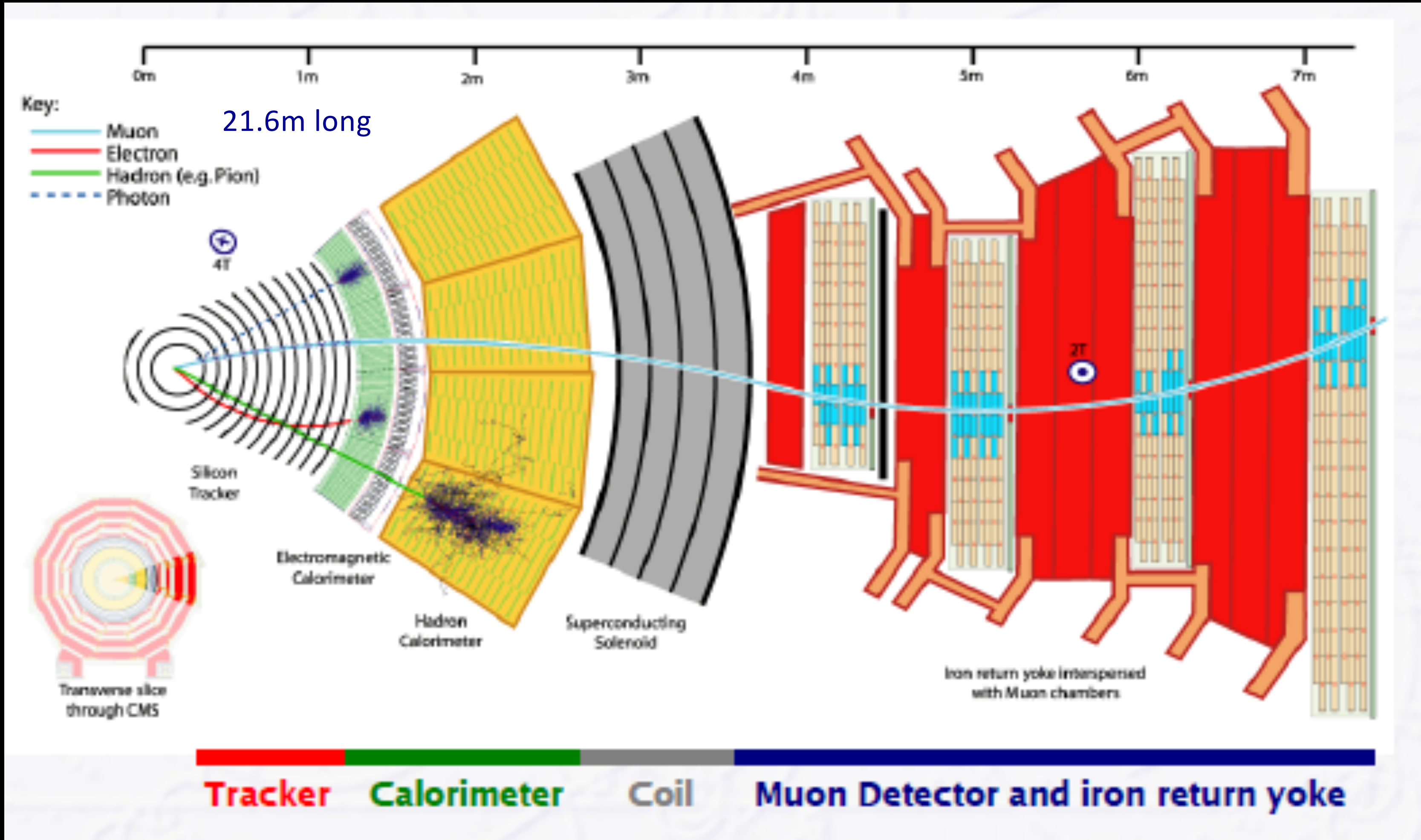

Silicon in the LHC Detectors

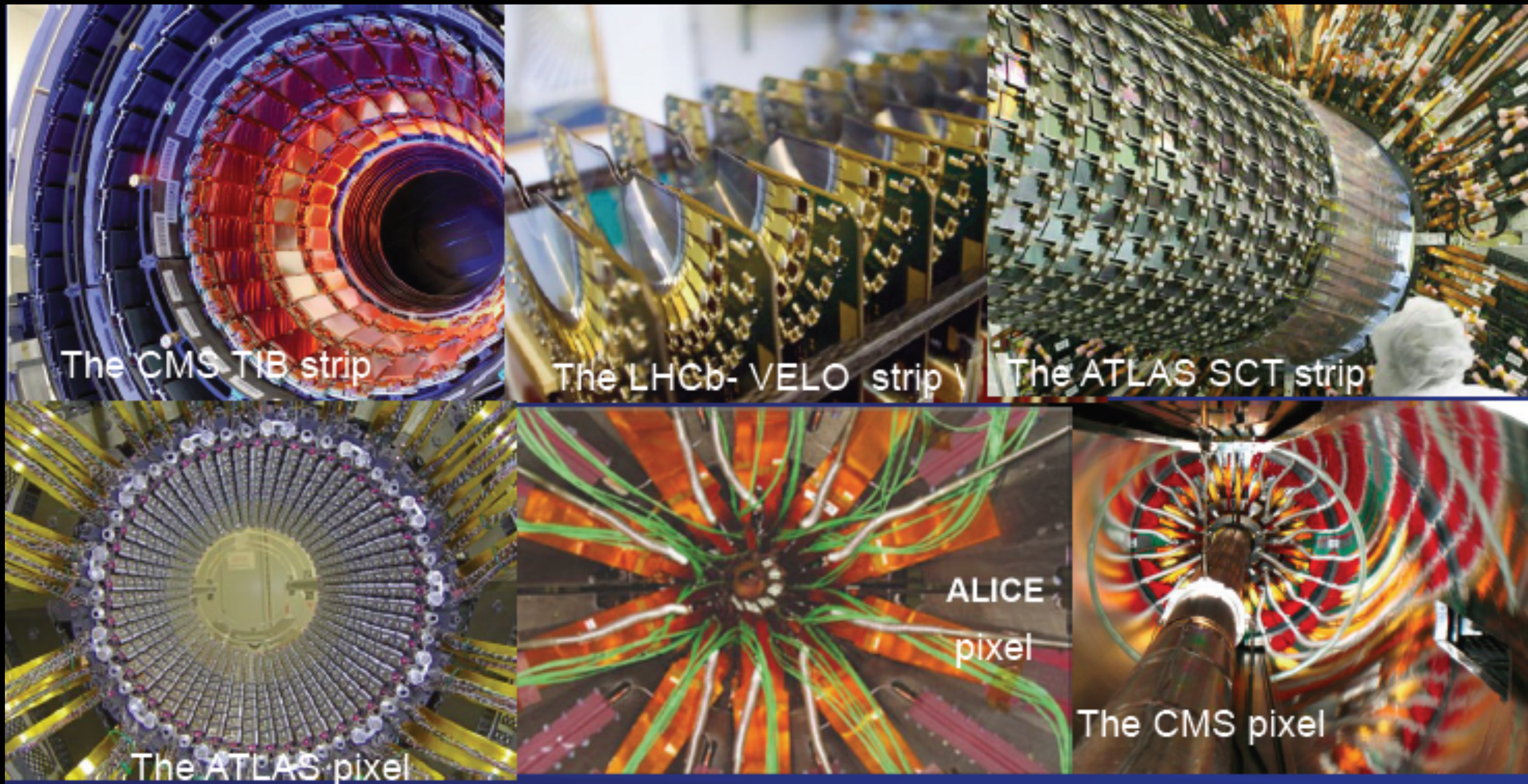

Cinzia Da Via, Uni. Manchester IEEE NPSS Workshop on Applications of Radiation Instrumentation, 2020

MANCHESTER 1824

ATLAS and CMS use alone more that 250m^2 of Silicon Strips to "image" charged particles

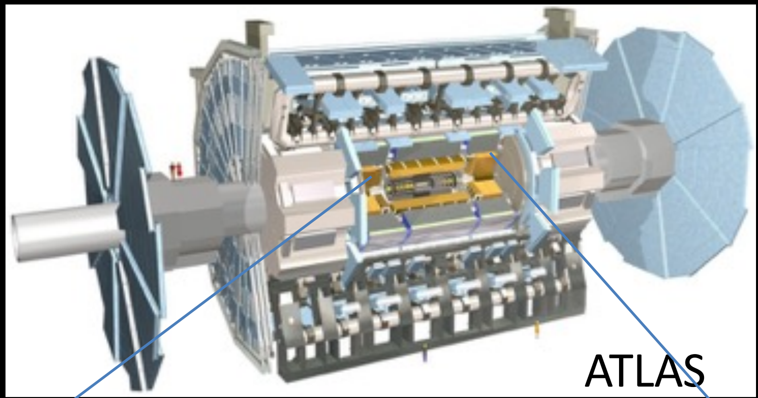

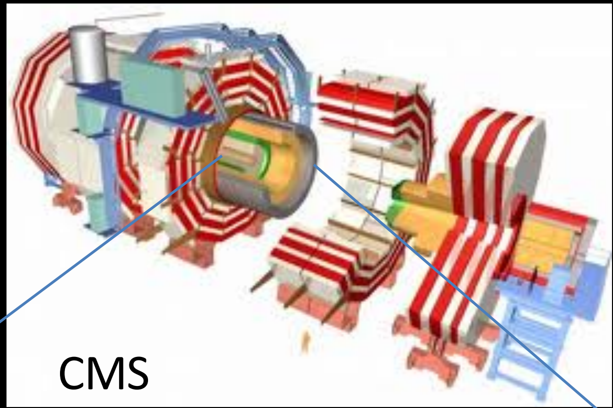

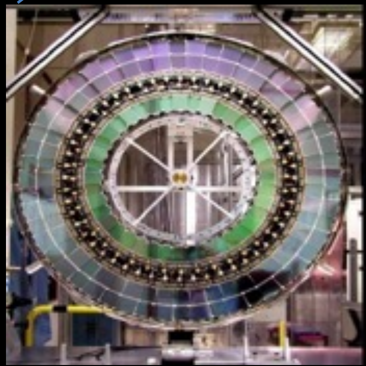

Strips
61m^2 of silicon.
6.2million channels 4 barrel layers + 9 disks per endcap
30cm < R < 52cm

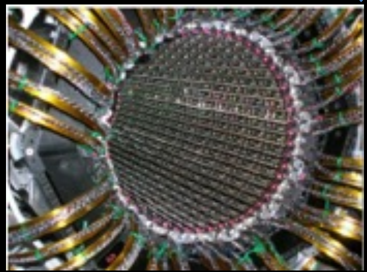

Pixels
3 Barrel layers
(r=5,9,12 cm)
2 end caps each with 3 disks
80Mpixels
50x400um2
Digital I/O

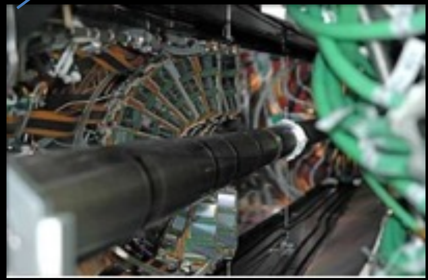

Pixels
3 barrel layers
2 end caps each with 2 disks
66 Mpixels 150 x 100um2
Analog I/O

Strips
198 m^2 of silicon,
9.3 million channels
Inner : 4 barrel layers,
3 end-cap disks
Outer: 6 barrel layers,
9 weels
22cm < R < 120cm

Cinzia Da Via, Uni. Manchester IEEE NPSS Workshop on Applications of Radiation Instrumentation, 2020

MANCHESTER 1824

Application1: Tracking Detectors

- Separate tracks by charge and momentum
- Position measurement layer by layer:

Inner layers: silicon pixel and strips → presence of hit determines position

Outer layers: strips or "straw" drift chambers → need time of hit to determine position

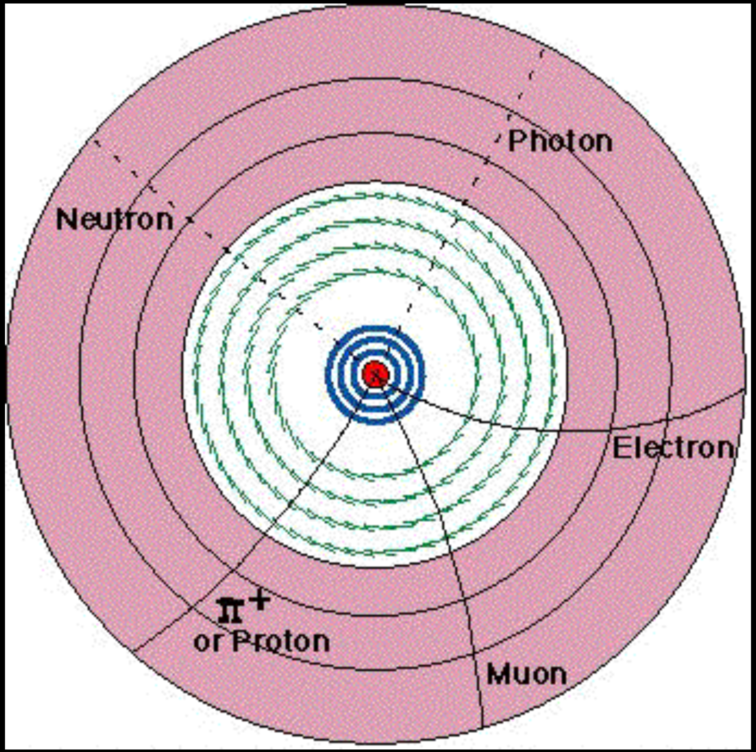

Example: Identification of Event Vertices

- primary event vertex reconstruction crucial in multiple collision events
- secondary vertices for live time tagging
- b- jet tagging

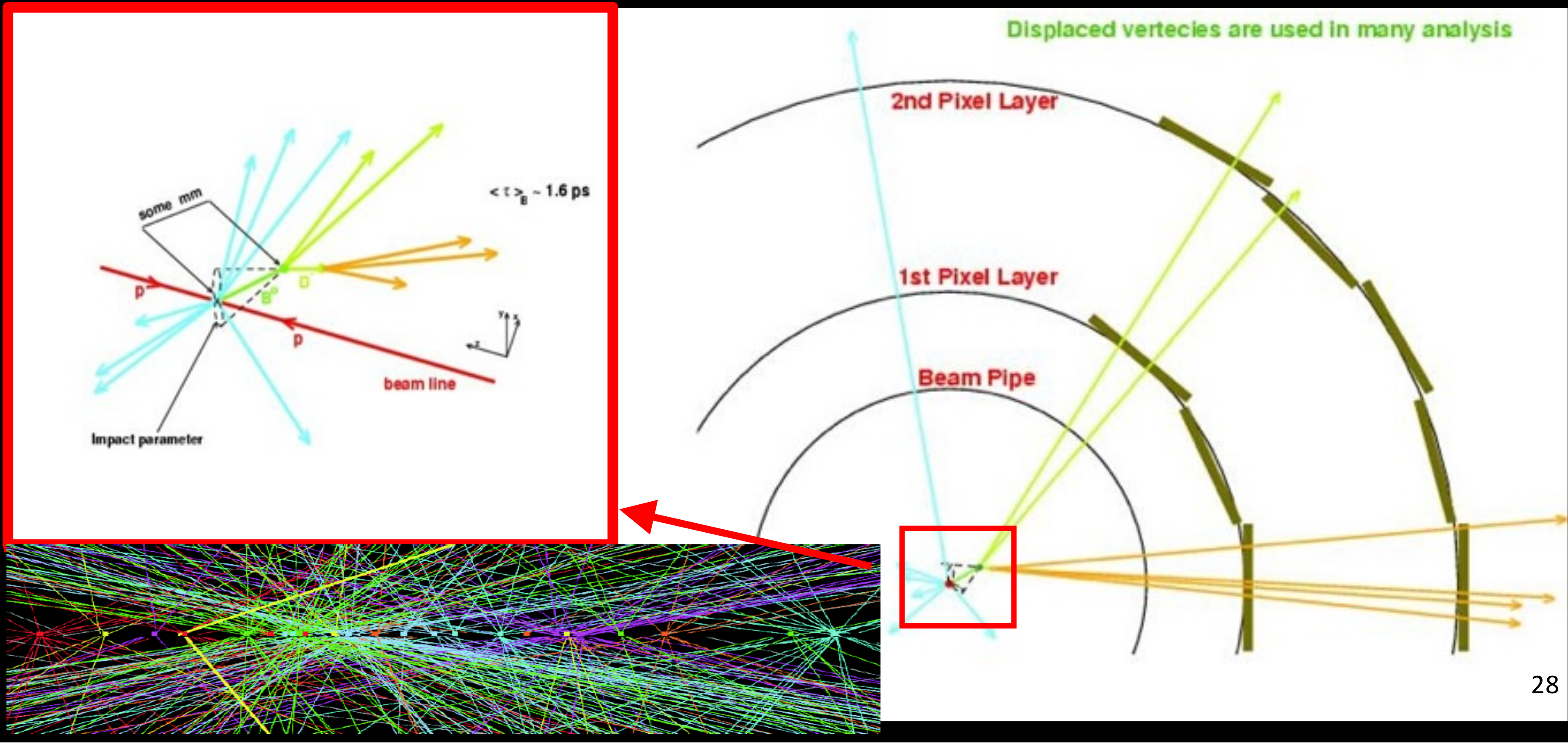

LHCb VErtex LOcator (VELO)

Search for physics beyond the Standard Model: CP-violation and rare decays of heavy hadrons

C. Farinelli

MANCHESTER 1824

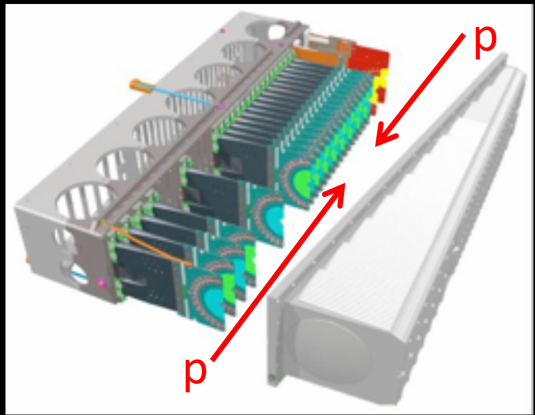

VELO characteristics:

- silicon sensors in secondary vacuum
- shielded by 300 μm RF foil
- 172,032 channels in total
- operating temperature of cooling system = -8°C

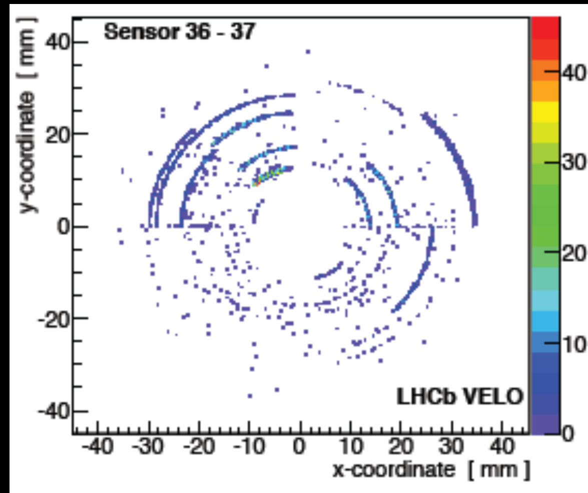

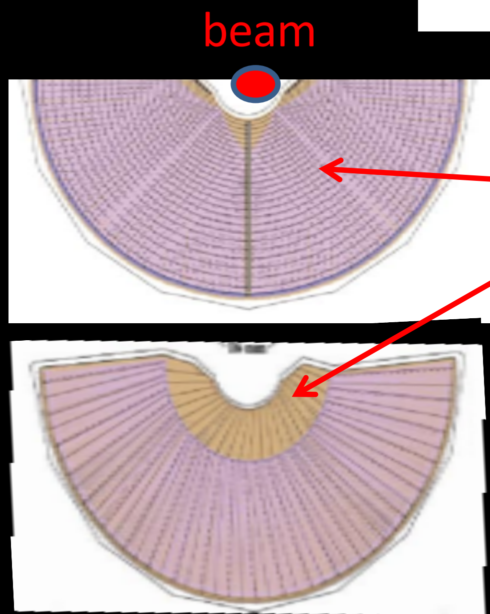

Silicon sensors with R-strips and φ-strips (2048 strips per sensor)

Sensor characteristics:
- 300 μm thick
- 8mm < radius < 42.2mm
- 40 μm < pitch < 101.6 μm
- radiation hard design:
- oxygenated silicon
- n-on-n type

TOTEM Roman Pots

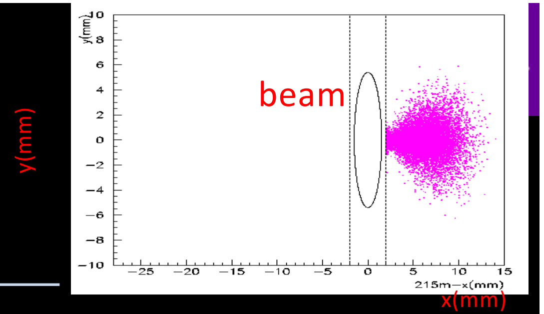

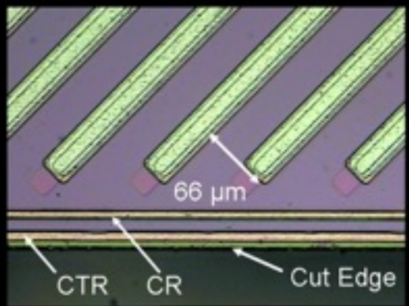

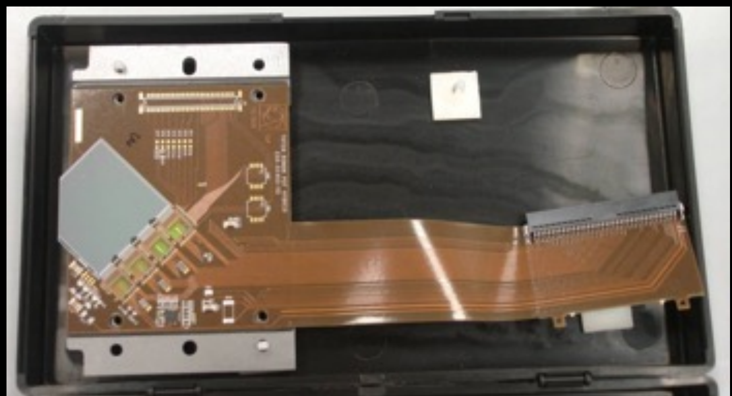

Totem measures the elastic scattering and the Total Cross Section at the LHC.

- Roman Pots are inserted in the beam pipe at 140-170m from the CMS experiment on both sides

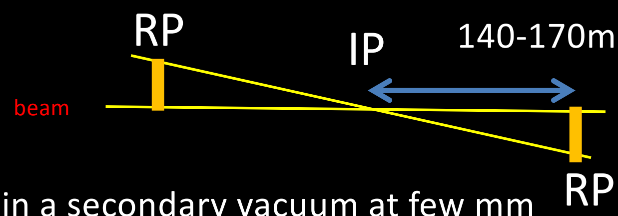

- Standard planar technology is placed in a secondary vacuum at few mm from the beam

- Edge width 50um at few mm from the beam

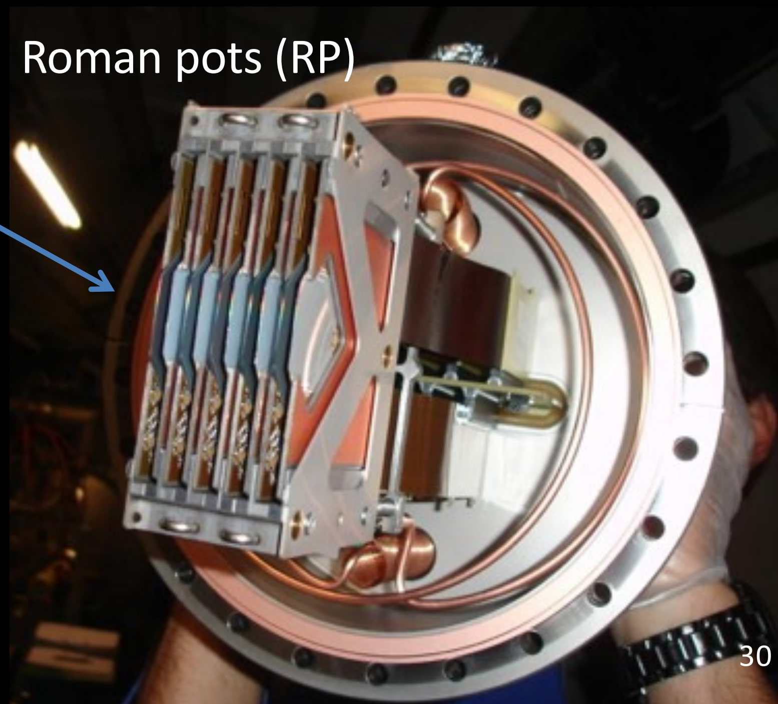

ALICE silicon drift detectors

study of heavy-ion collisions at the LHC

MANCHESTER 1824

G. Batigne IFAE

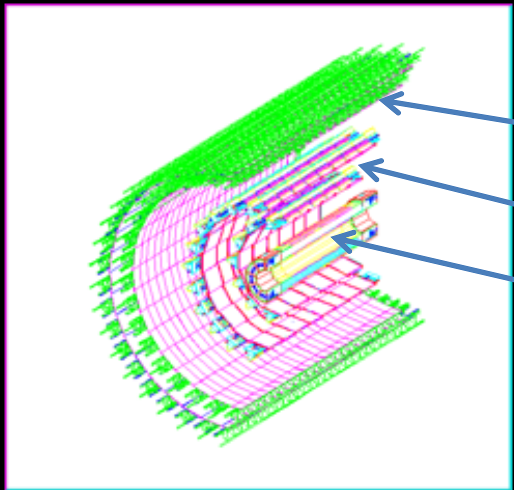

Position reconstruction : Centroid calculation
Position X : anods n+
Position Y : drift time (calibration of Vdrift)
dE/dx : Integral of the signal

Very low C and therefore very low noise!

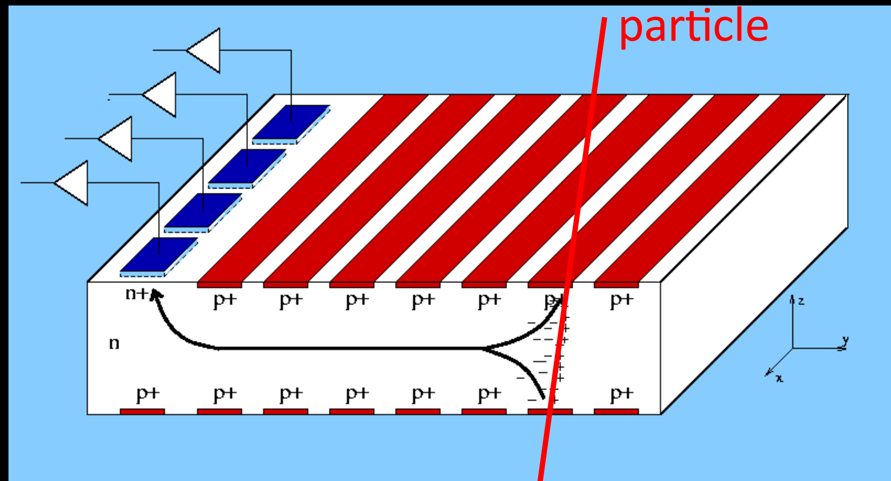

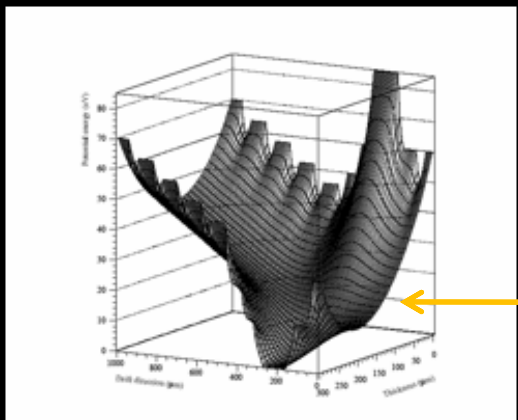

p+ cathods on both side of the wafer :

- Depletion of the Silicon
- HV decreases toward the n+ anods

Drift field (Toboggan effect)

Last cathods below anods :

- kick-up voltage

LGAD Basics. Low Gain Detector

G. Pellegrini, Low Gain Avalanche Detectors

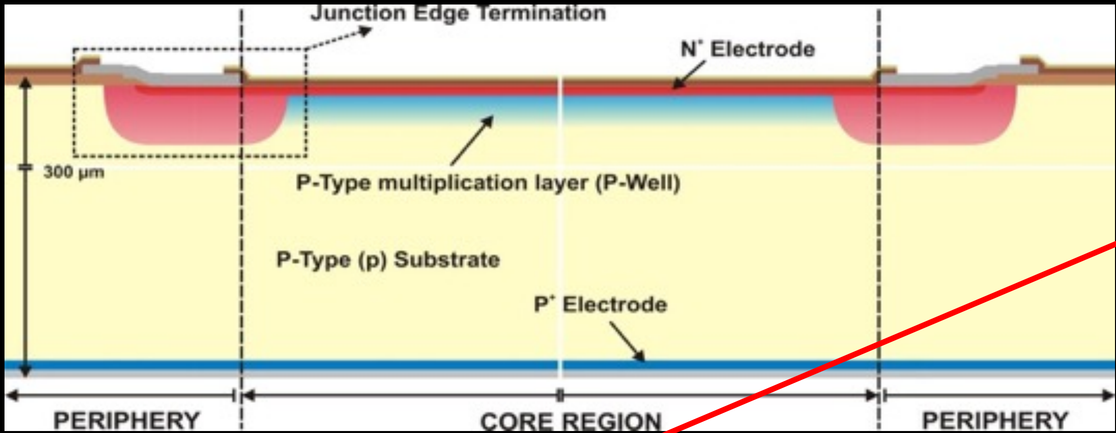

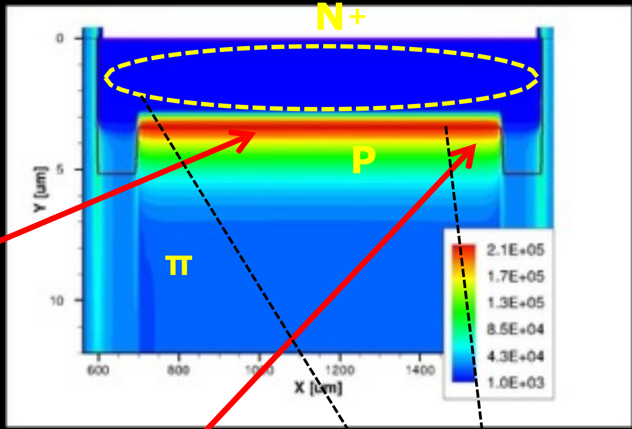

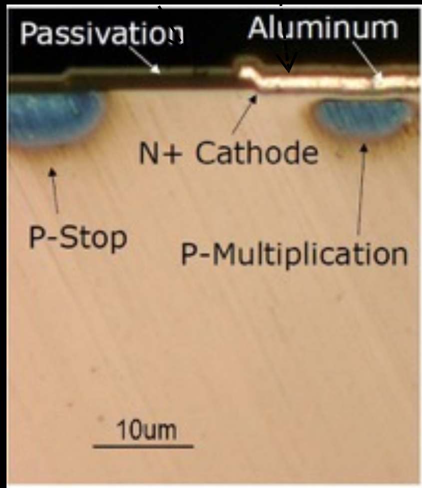

- **Core Region**
  - ✓ **Uniform electric field**, high enough to activate mechanism of **impact ionization** (multiplication)
- **Termination**
  - ✓ **High electric field** confined in the **core region**
- **Periphery**
  - ✓ **Dead region**. **Charges** should not be collected. **Reduction** of the surface **leakage currents**

LGAD Measurements

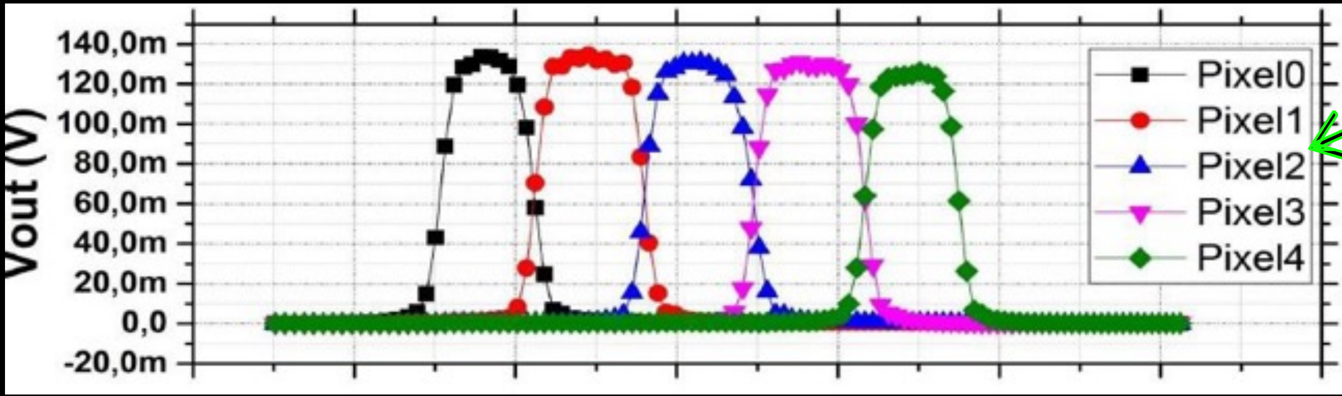

O. Alonso et al., presented at the PIXEL2016 workshop.

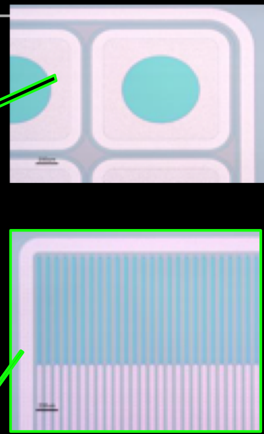

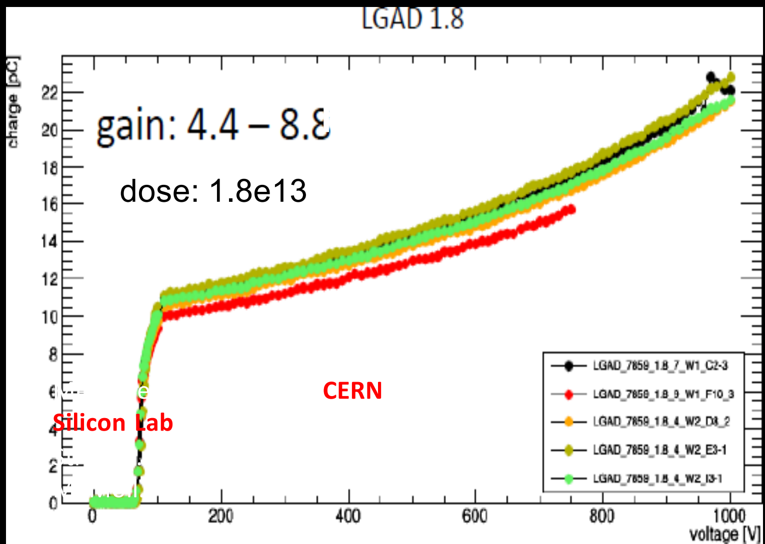

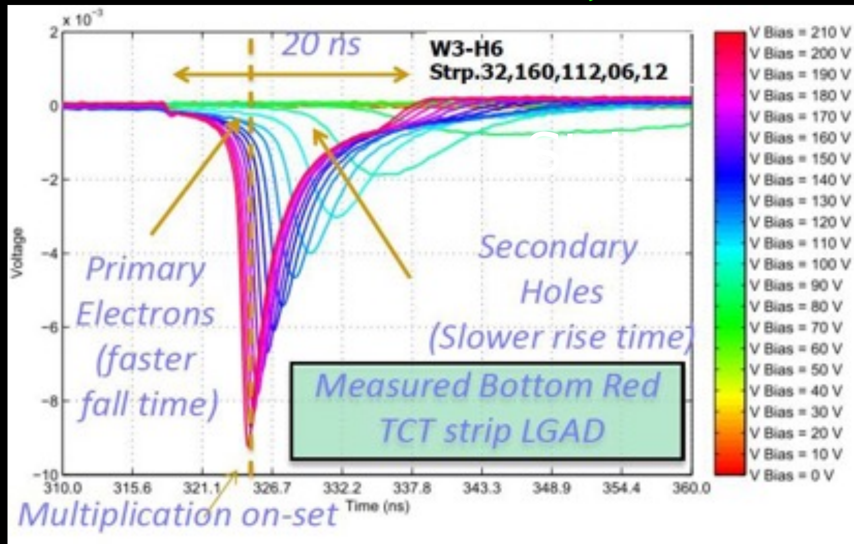

I. Vila, presented at the 28th RD50 workshop

What happens during irradiation to silicon detectors?

Defects formation in irradiated silicon

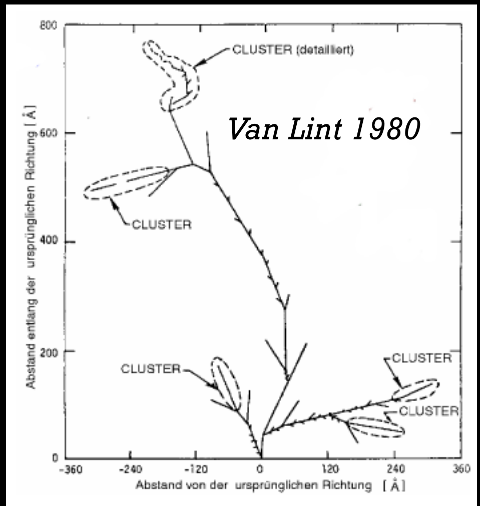

Primary Knock on Atom

Displacement thresholds in Si:
Frenkel pair E~25eV
Defect cluster E~5keV
For X-Rays E~250KeV

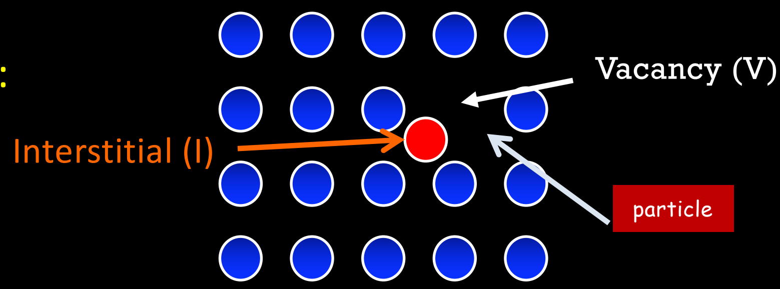

V, I MIGRATE UNTIL THEY MEET IMPURITIES AND DOPANTS TO FORM STABLE DEFECTS

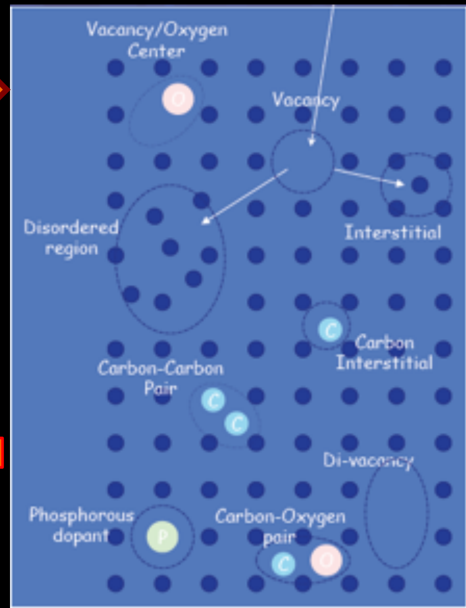

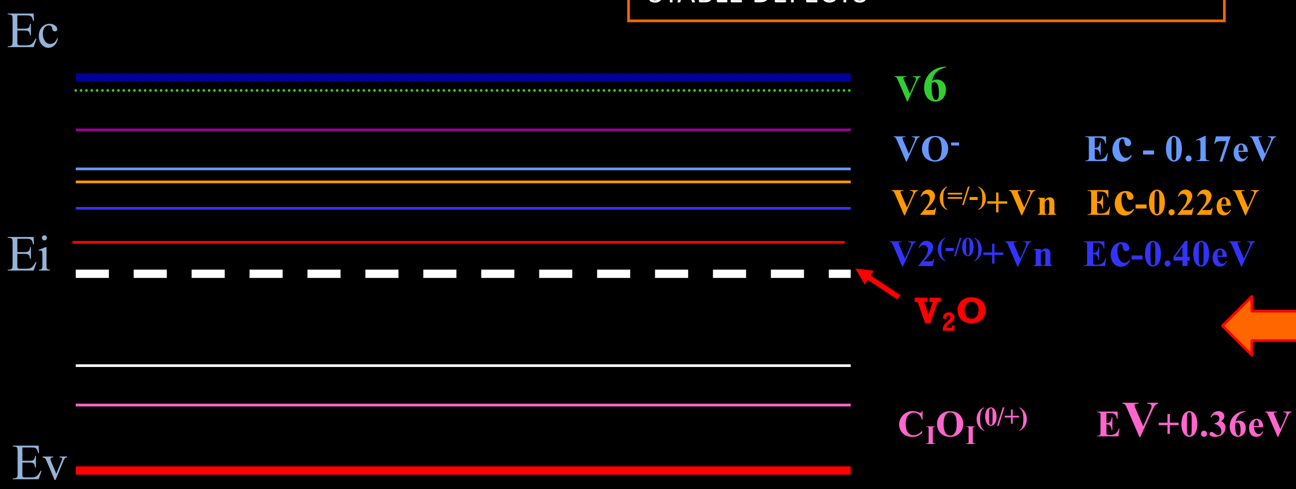

Defects position in the bandgap

3D radiation sensors

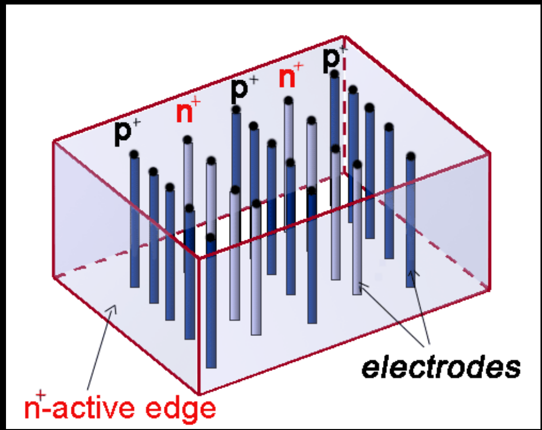

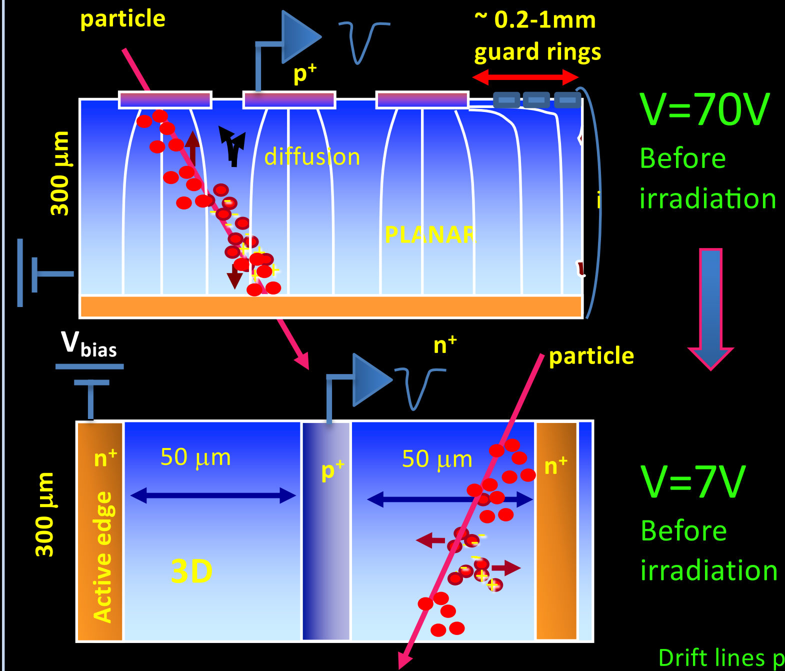

Drift lines parallel to the surface

3D silicon detectors were proposed in 1995 by S. Parker, and active edges in 1997 by C. Kenney.

Combine traditional electronics processing and MEMS (Micro Electro Mechanical Systems) technology.

Electrodes are processed inside the detector bulk instead of being implanted on the wafer's surface.

The edge is an electrode! Dead volume at the edge < 5 microns!

The electric field is parallel to wafer’s surface: and smaller inter-electrode spacing: low bias voltage, low power, reduced charge sharing and high speed – for the same wafer thickness

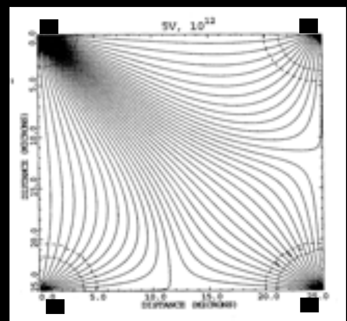

MEDICI simulation of a 3D structure

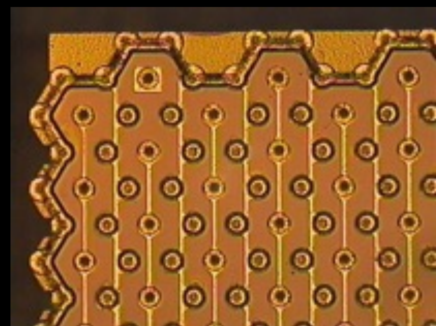

3D is "geometrically" radiation hard at low V_{bias} (hence low power)

Ramo's theorem

$$\lambda = v_D \cdot \tau$$

$$S = \frac{\lambda}{L}\left[1 - \exp\left(-\frac{x}{\lambda}\right)\right]$$

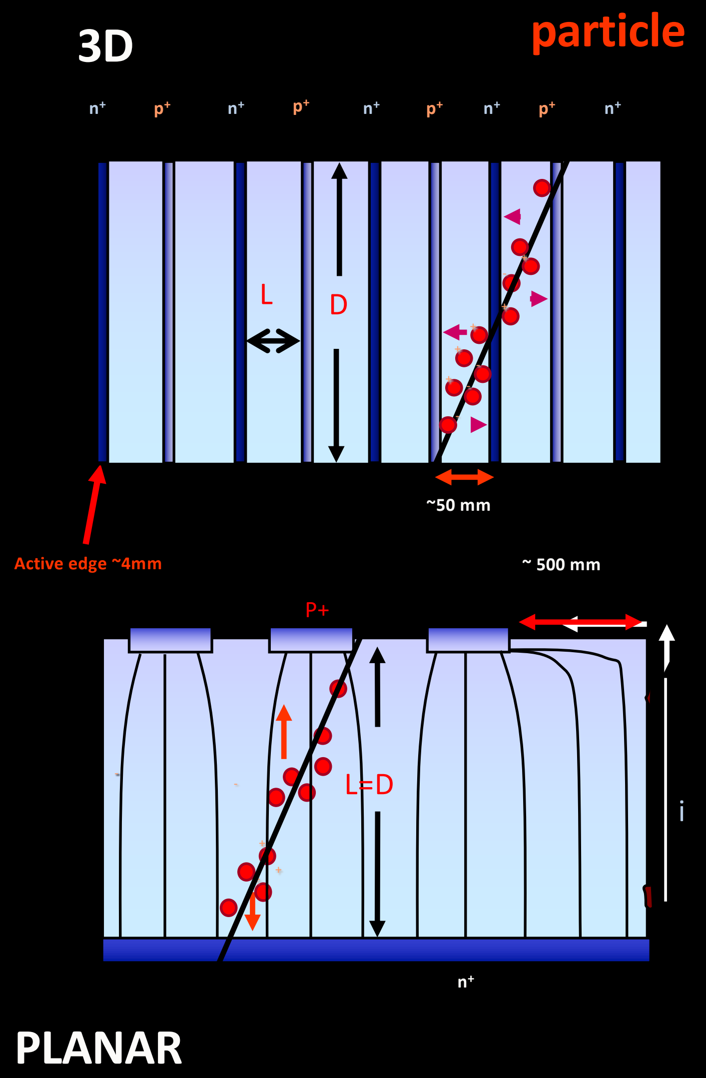

3D 4E
3D 3E
3D 2E
Diamond
Thick Si
Thin Si

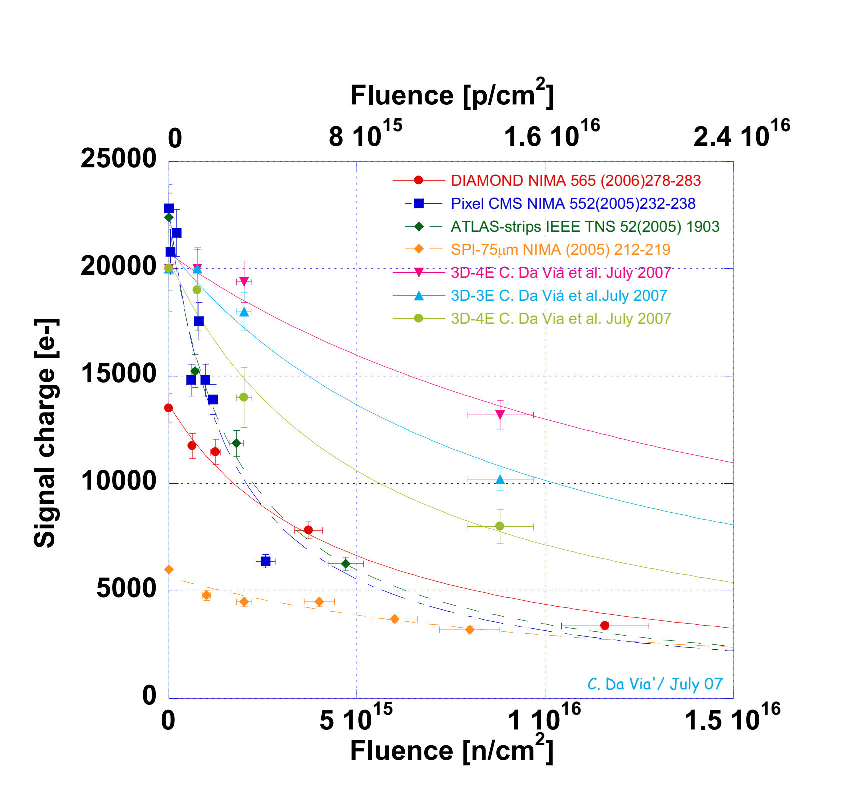

NIM A 603 (2009) 319–324

3D Speed Properties

3D Tests with 0.13 mm CMOS Amplifier chip
(A Kok, S. Parker, C. Da Viá, P. Jarron,
M. Depeisse, G. Anelli), fabricated at Stanford
By J. Hasi, C. Kenney

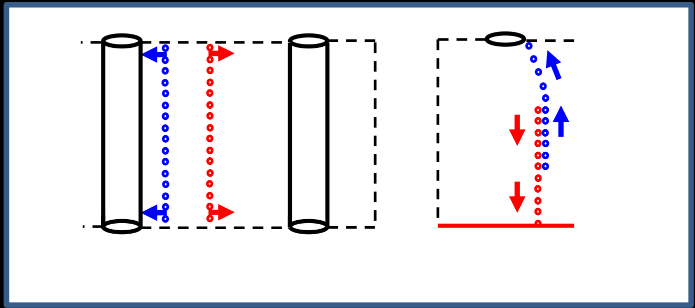

- Short collection distance
- High average e-field at low V_{bias}
- Parallel charge collection

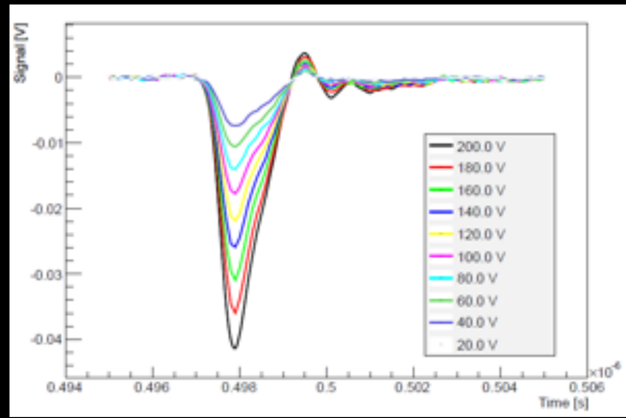

After irradiation $2x10^{16}ncm^2$

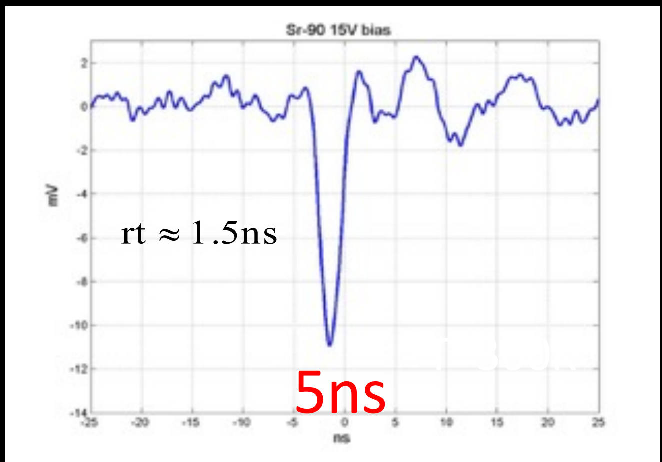

Raw oscilloscope Trace rt is dominated by amplifier

3D Inter-electrode spacing = 56 um

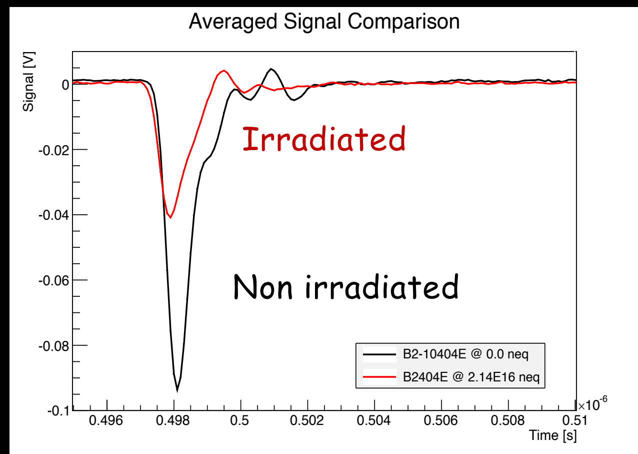

3D with small IES and trench electrodes

Slide from A. Lai TIMESPOT collaboration

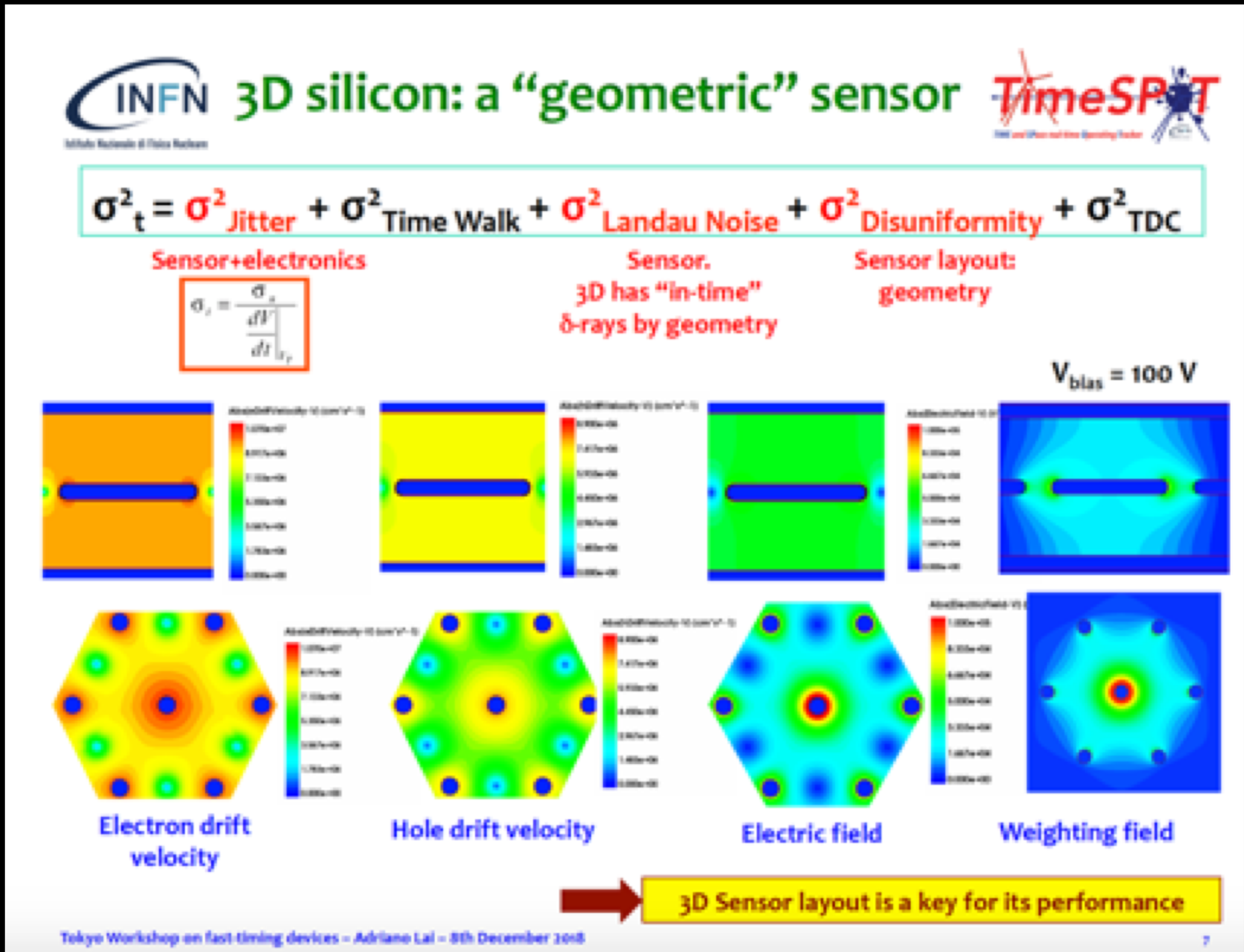

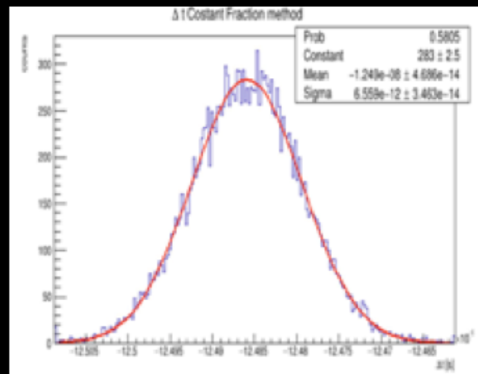

1030 nm laser, single spot, 1 MIP equiv. charge deposit

$\sigma_t \approx 6.5$ ps

MANCHESTER 1824

The key to fabrication: plasma etching

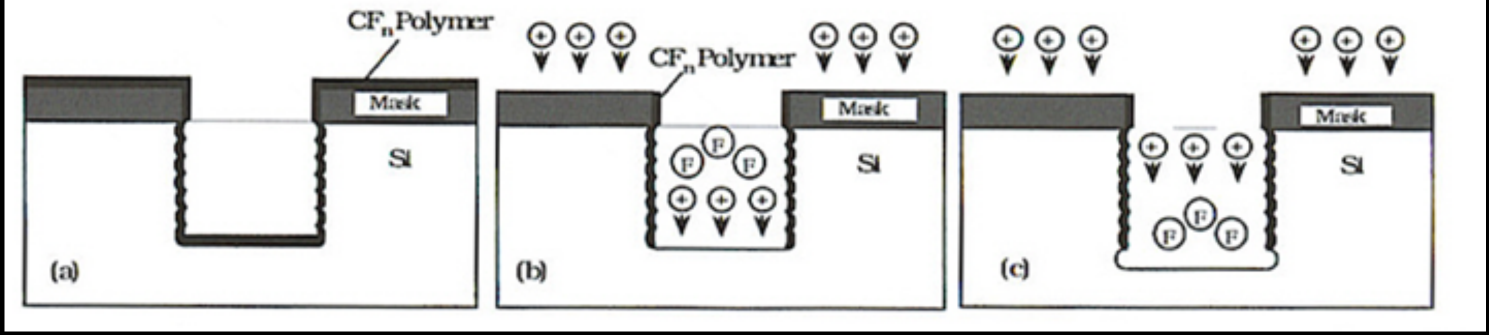

BOSCH PROCESS: alternating passivation (C_4F_8) and etch cycles (SF_6);

- Within the plasma an electric field is applied perpendicular to the silicon surface.
- The etch cycle consists of fluorine based etchants which react with silicon surface, removing silicon. The etch rates are ~1-5µm/minute.
- To minimize side wall etching, etch cycle is stopped and replaced with a passivation gas which creates a Teflon-like coating homogenously around the cavity. Energetic fluorine ions, accelerated by the e-field, remove the coating from the cavity bottom but NOT the side walls.

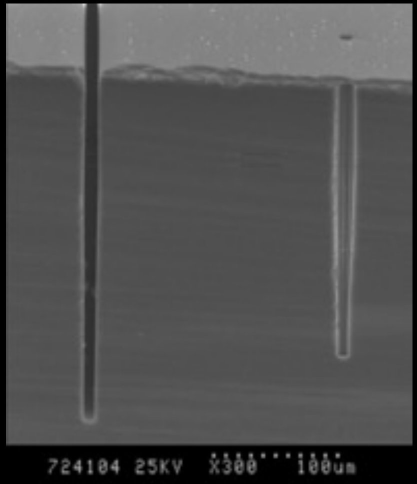

Slide from J. Hasi

Existing 3D designs

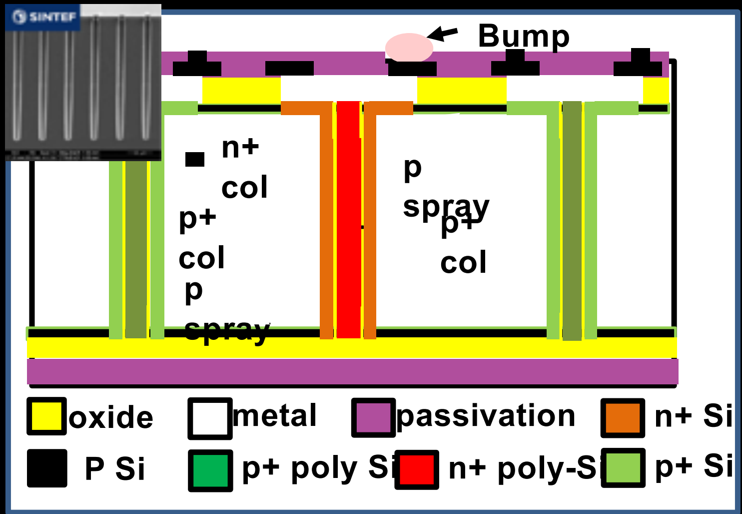

Single side, full 3D with active edges requires a support wafer which is removed later

Double sided full or partially through3D with slim-fences (~200um)

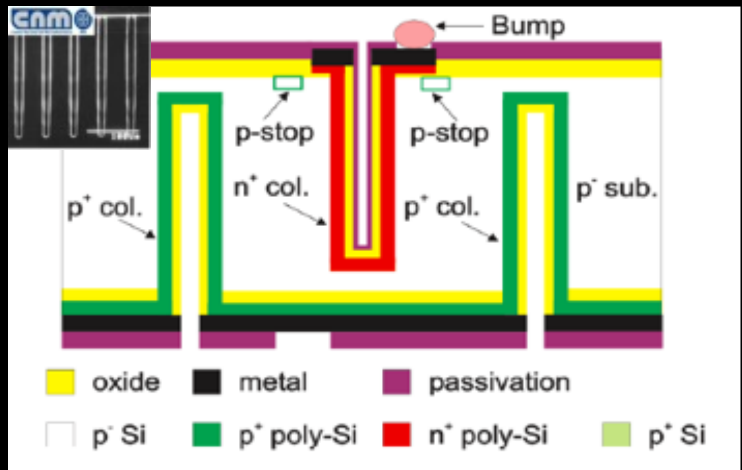

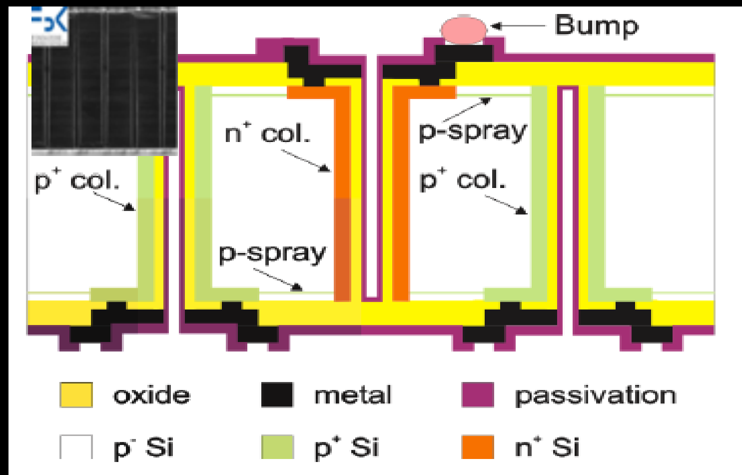

3D sensors are installed in the LHC since 2014
Upgrade in the ATLAS –Insertable B-Layer (IBL)
>300 sensors fabricated and now being loaded to cover 25% IBL

MANCHESTER 1824

NIMA 694 (2012) 321–330

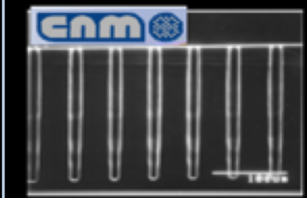

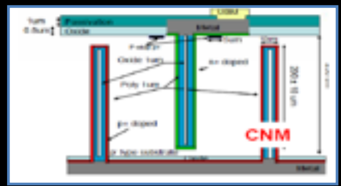

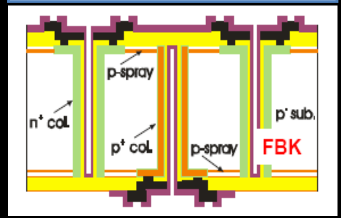

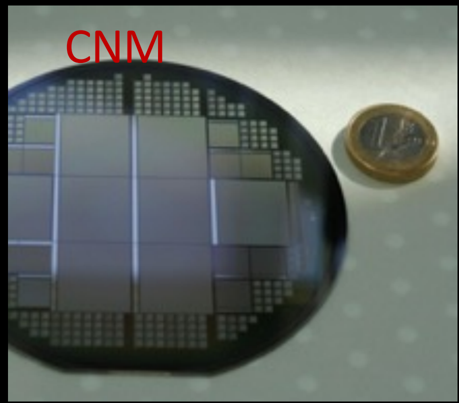

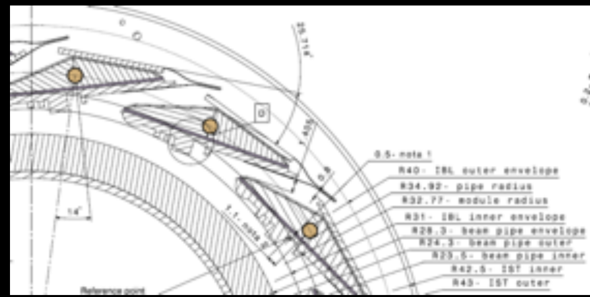

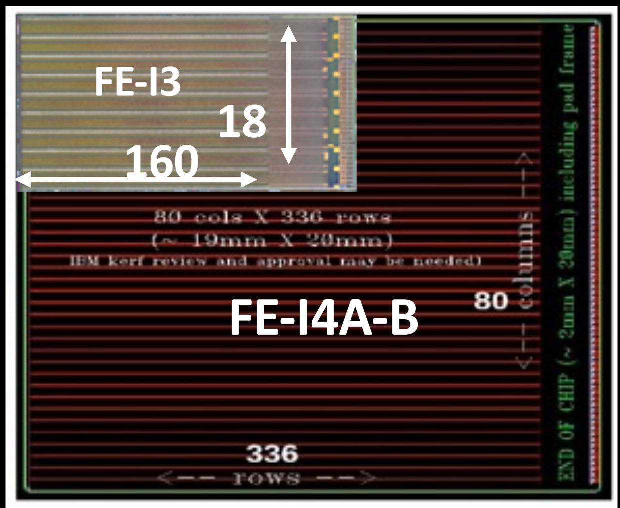

2x2cm2
250x50um2, 26880 pixels

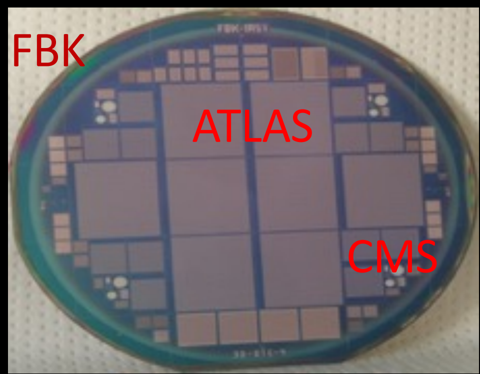

SINTEF
ITC irst
FONDAZIONE BRUNO KESSLER
cnm

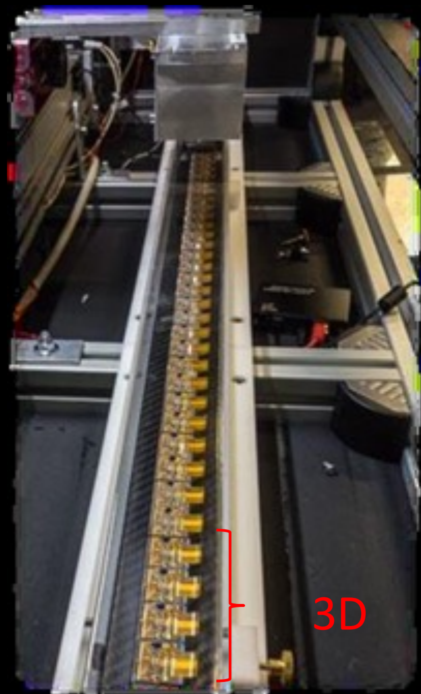

"3D" Radiation Detectors and Active Edges

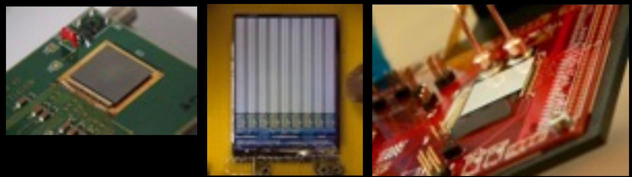

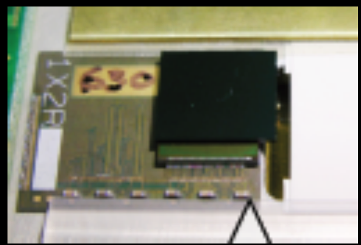

ATLAS FE-I3
ATLAS FE-I4 (with micro-channels)
AFP
Medipix/Timepix
CMS

LHC-Upgrades

- GaAs
- CdTe
- Diamond

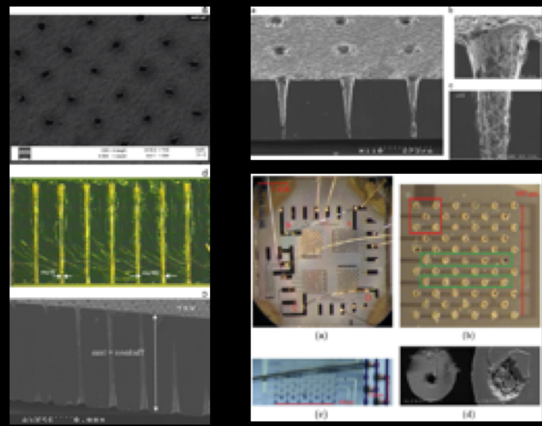

Silicon +ASIC

Consolidated

Silicon +Converter

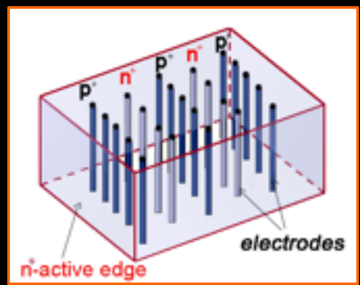

New Materials

Emerging

New Shapes

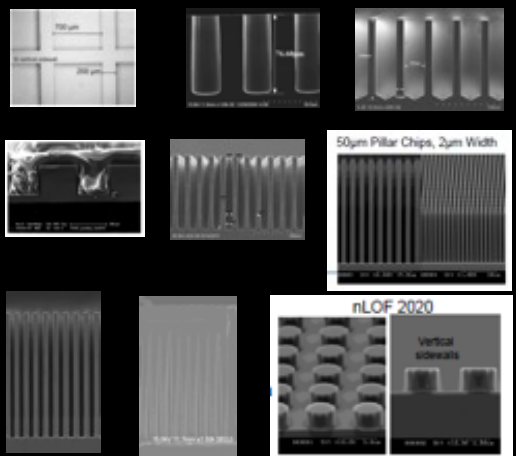

Neutron detectors

3D

Very fast!!

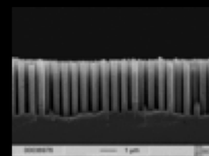

- Core shell
- Trench
- Curved
- Edge
- Ring..

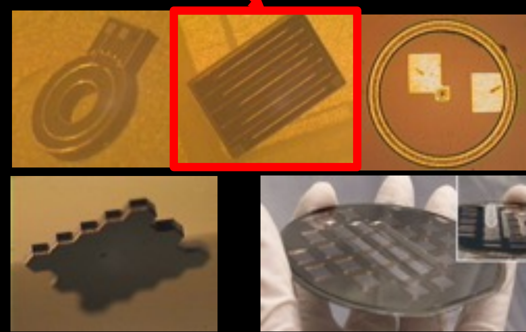

3D Vertically Integrated Module with CO2 internal cooling

C. Da Via, F. Munoz-Sanchez, N. Dann,
D. Hellesmidht, P. Petagna, G. Romagnoli
Paper in preparation

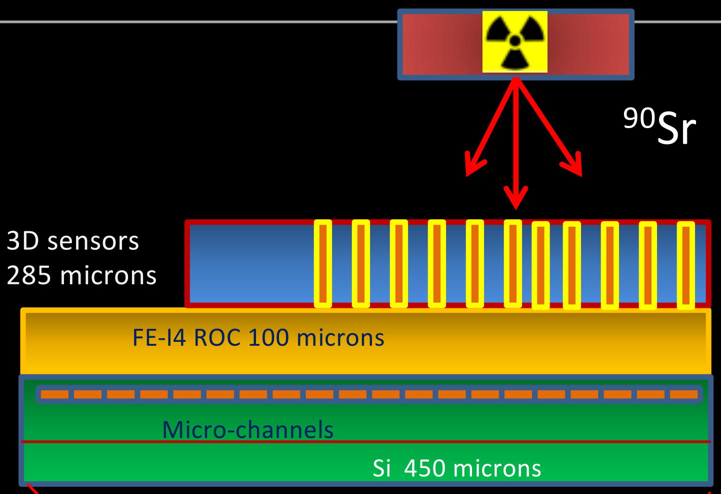

- 3D silicon : CNM double side 285 um thick IBL qualification batch
- FE-I4A: thinned to 100um at IZM
- Si-Si micro-channels
  designed by CERN PH-DT,
  produced by PH-DT in EPFL CMi cleanroom,
  direct bonding CSEM
- Glue: 2-components
  Masterbond EP37-3FLFAO

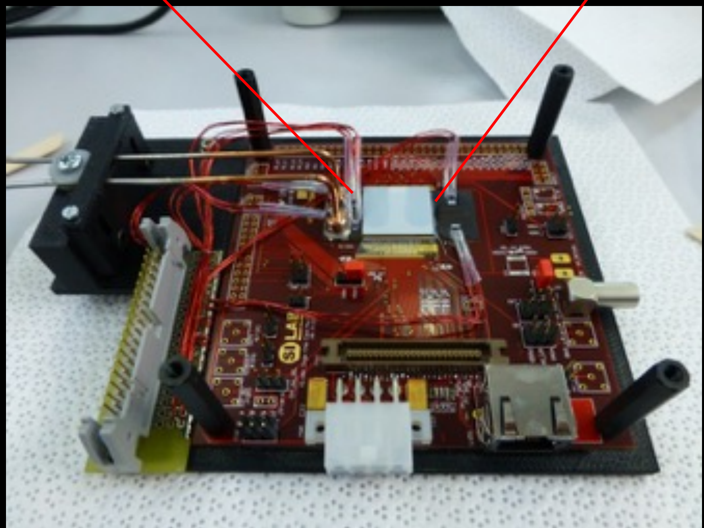

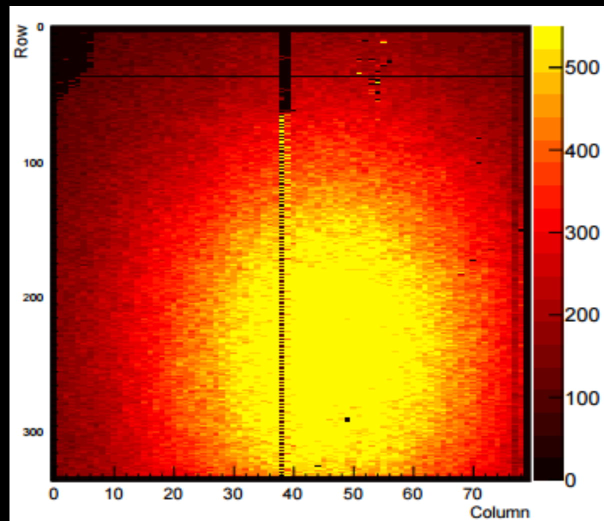

MANCHESTER 1824

Applications: High Efficiency Neutron Detection

Uher et al. Nuclear Instruments and Methods in Physics Research A 576 (2007) 32–37

- Silicon is not sensitive to neutrons but is a well known radiation detector
- Need neutron reactive converter materials usually deposited on the surface thin films or different geometries
- With reference to ^{10}B converter:
  - 90% capture in 43 µm
  - Range of reaction products 2-5 µm

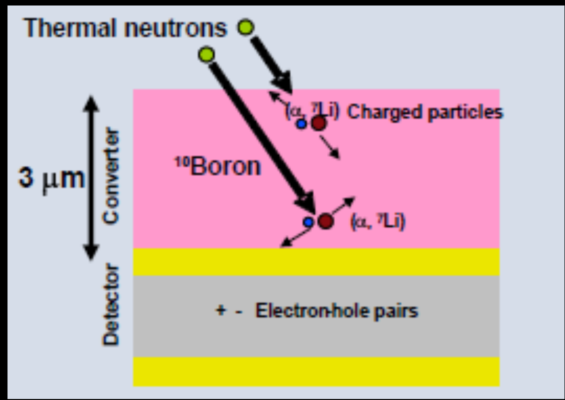

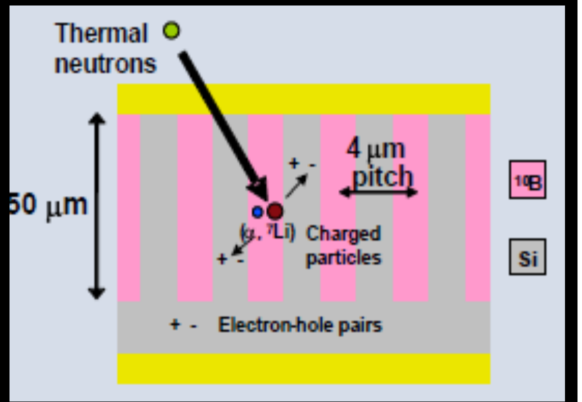

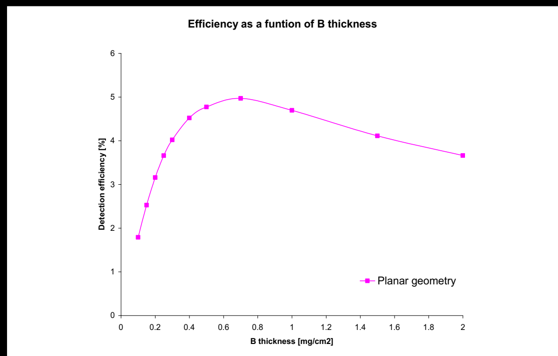

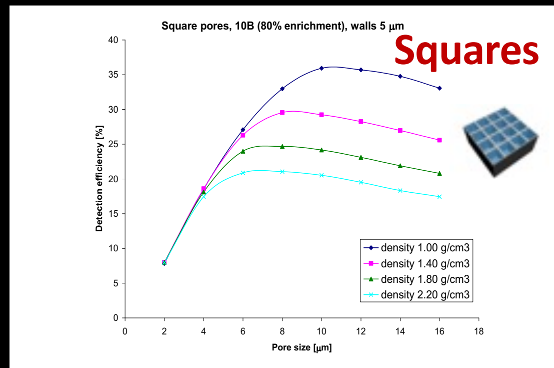

Amorphous ^{10}B, enrichment 80%
Efficiency < 5%

Efficiency up to 36%

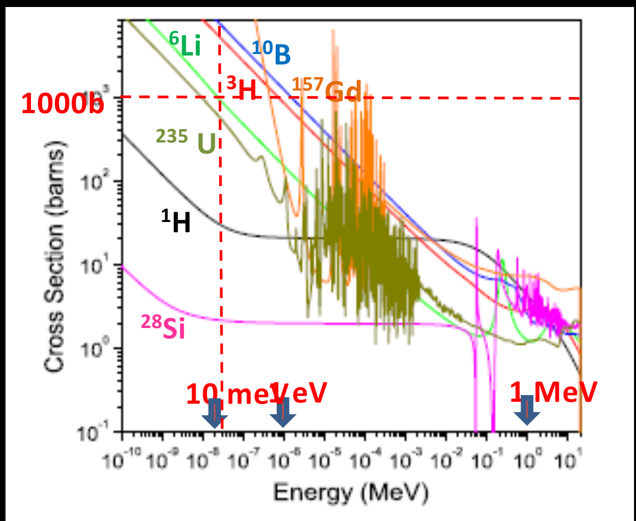

J. Phys.: Condens. Matter **22** (2010) 443201 (32pp)

Neutron cross sections of some common n-reactive materials

Micro-structured Semiconductor Neutron Detectors (MSND)

D. McGregor et al., J. Crystal Growth 379 (2013) 99

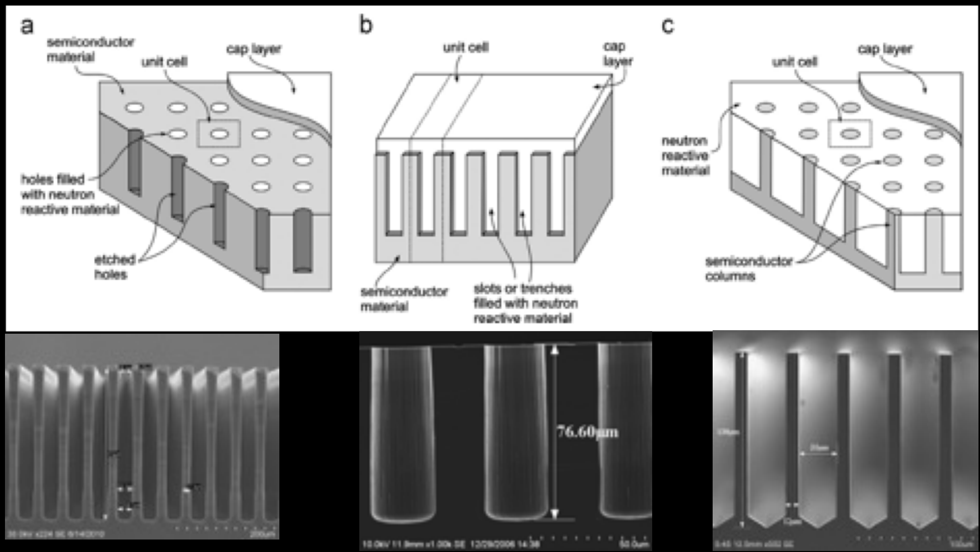

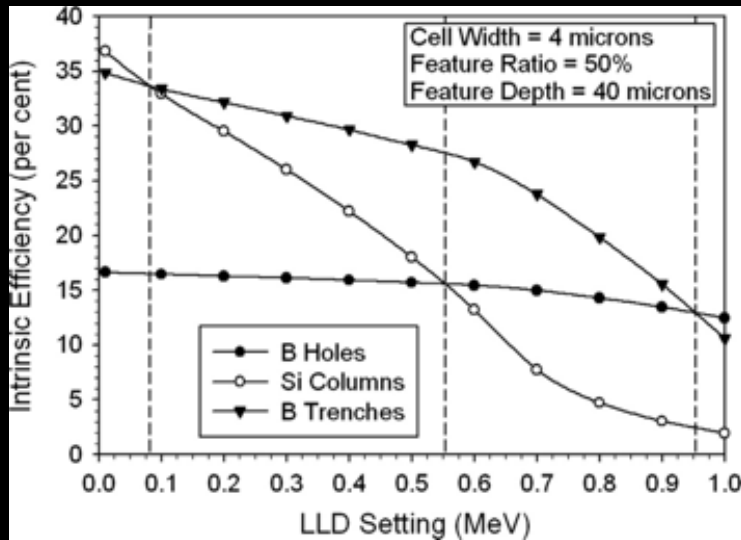

- Extended interaction surface, and higher probability for reaction products to enter the semiconductor
- Different shapes and geometries

Comparison of efficiencies as a function of feature size, as measured by its cell fraction, for hole, trench and column designs with unit cell dimensions of 4 um and feature depths of 40 um. ^{10}B is the back fill material and the LLD was set for 300keV

Maximum efficiencies reported ~50%

Applications: Detectors in Space

AMS (Alpha Magnetic Spectrometer) on ISS particle physics experiment in space to measure antimatter in cosmic rays

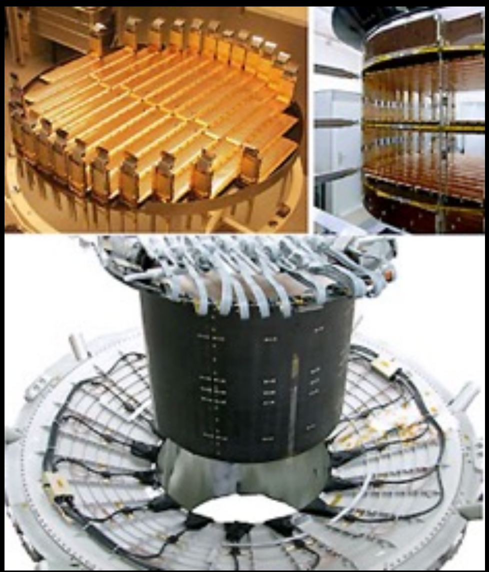

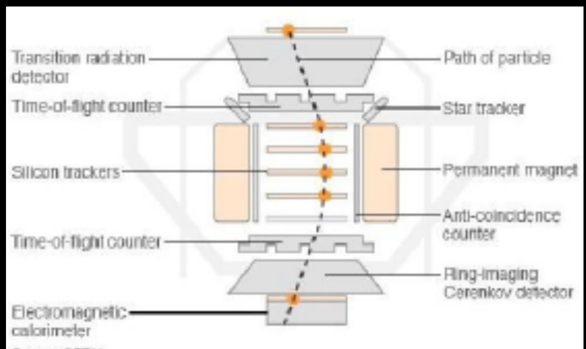

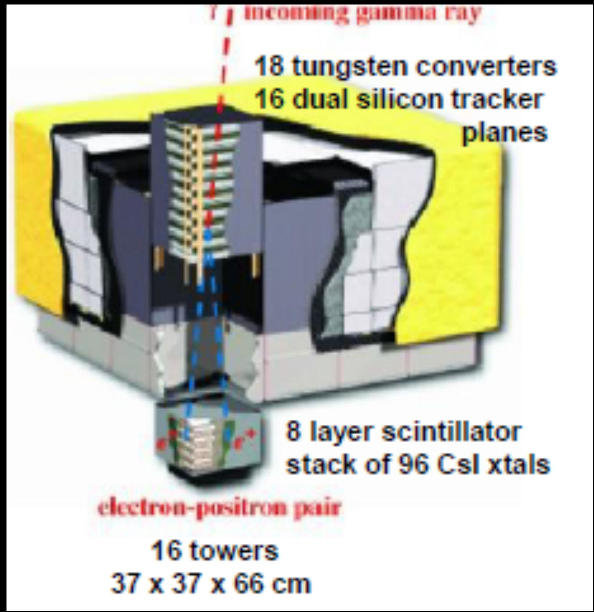

FERMI Large Area Telescope

Gamma-ray detector

Cycle of pulsed gamma rays from the Vela pulsar. Constructed from photons detected by Fermi's Large Area Telescope.

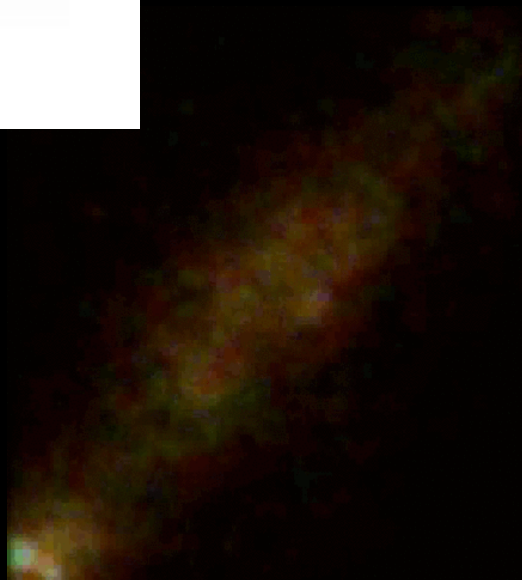

Roger Romani

Applications: Ground Detectors – Cosmic Rays

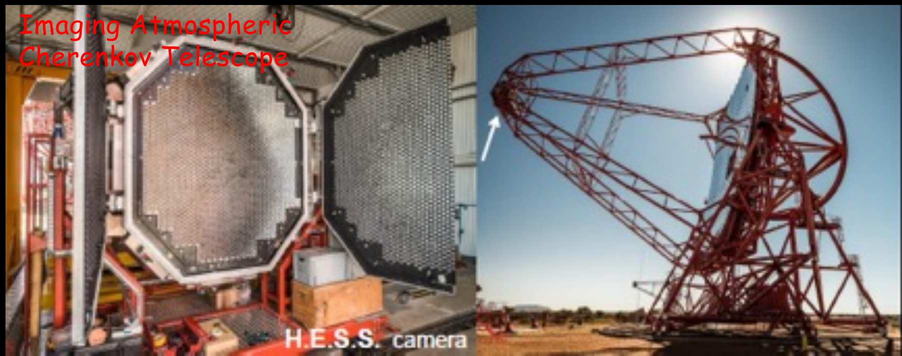

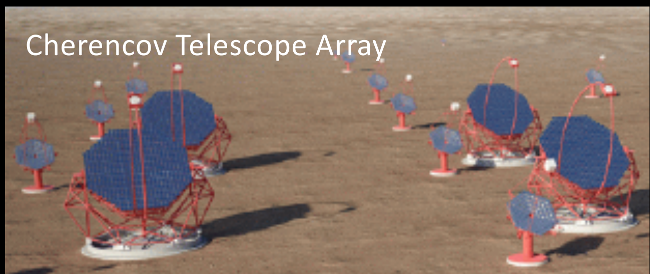

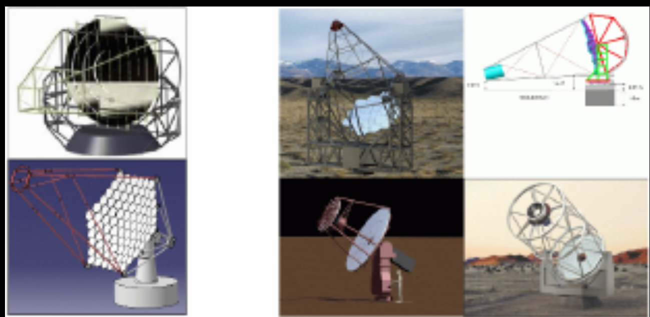

SST 70x (S) : > few TeV
>5 m², >8° FoV, <0.25° pxl

MST 25x (S) : 0.2-10 TeV
>88 m², >7° FoV, <0.18° pxl

LST 4x (S) : 20 GeV - 1 TeV
>330m², >4.4° FoV, <0.11° pxl size

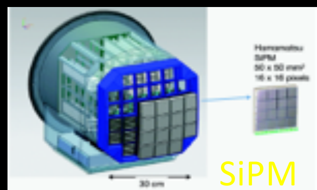

Camera Options

Pierre Auger Observatory

UHE 10^{20}eV
1600 water
Cherencov detectors

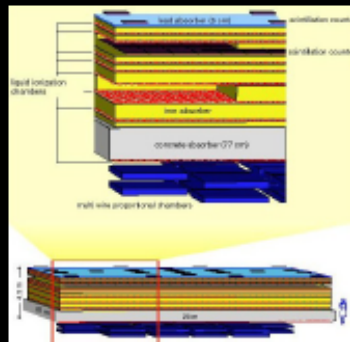

KASCADE-Grande

200x200 m² scint. array
20x16 m² h. calorimeter
128 m² muon tracker

ARGO-YBJ -RPCs

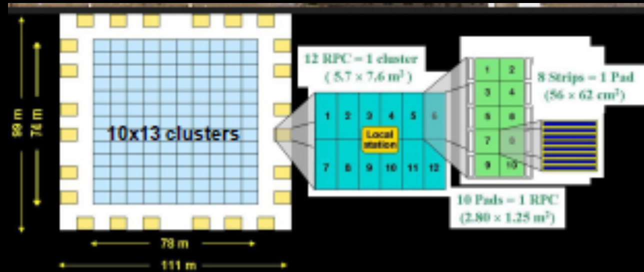

Follow-up project LHAASO

MANCHESTER 1824

Applications: Environmental Radiation Monitoring

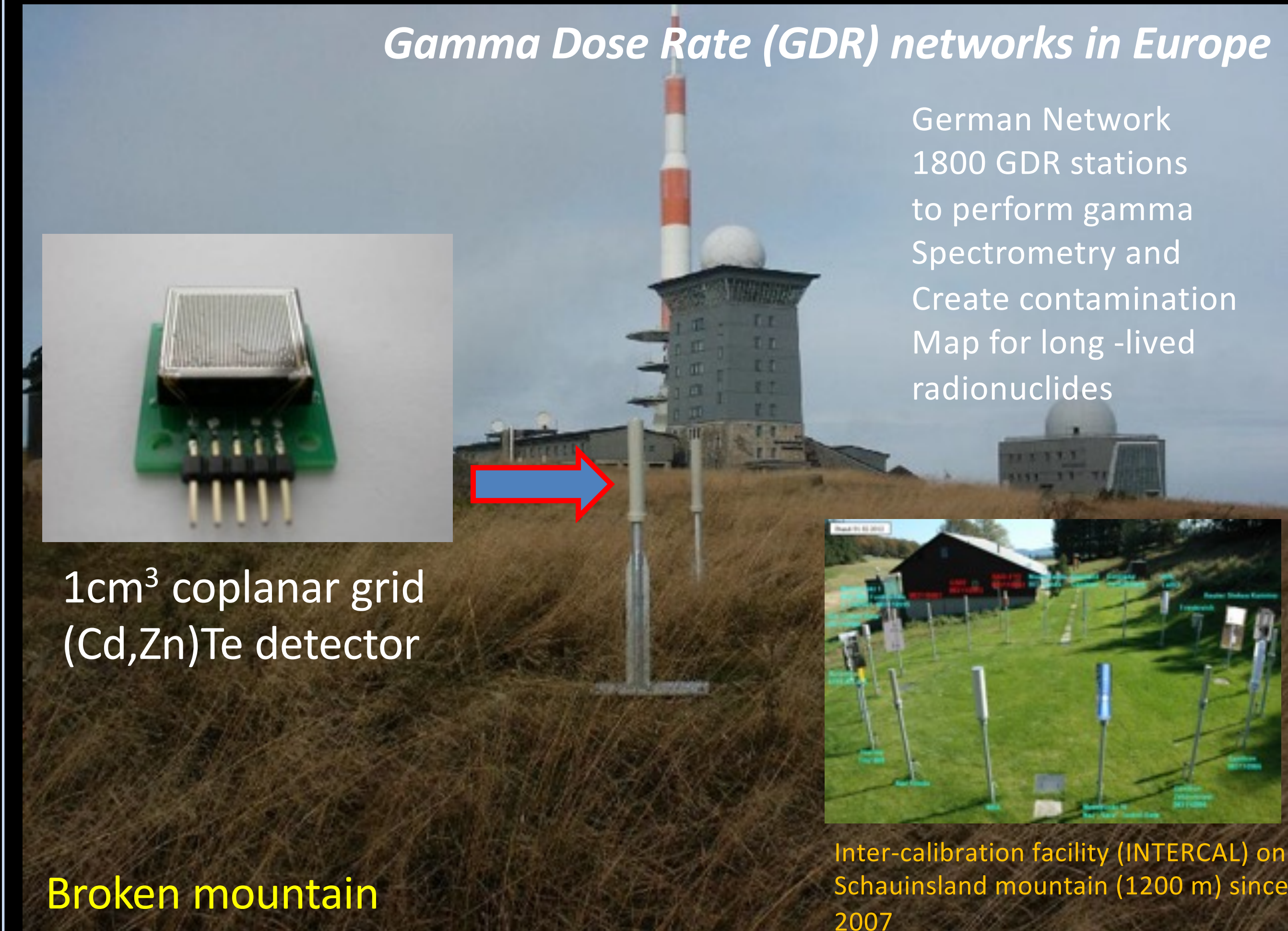

Gamma Dose Rate (GDR) networks in Europe

German Network
1800 GDR stations
to perform gamma
Spectrometry and
Create contamination
Map for long -lived
radionuclides

1cm^3 coplanar grid
(Cd,Zn)Te detector

Broken mountain

Inter-calibration facility (INTERCAL) on Schauinsland mountain (1200 m) since 2007

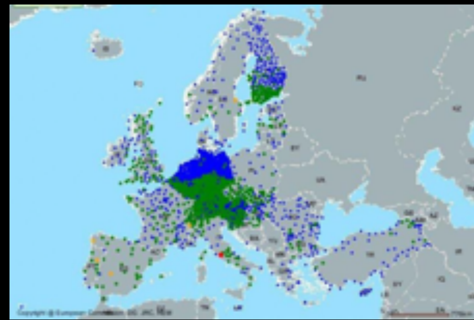

European countries established GDR networks during the cold war period and improved these networks after the Chernobyl accident in 1986.

Monitoring of:

nuclear facilities
atomic bomb scenarios
terroristic attacs

U. Stöhlker

Applications: Medical Imaging

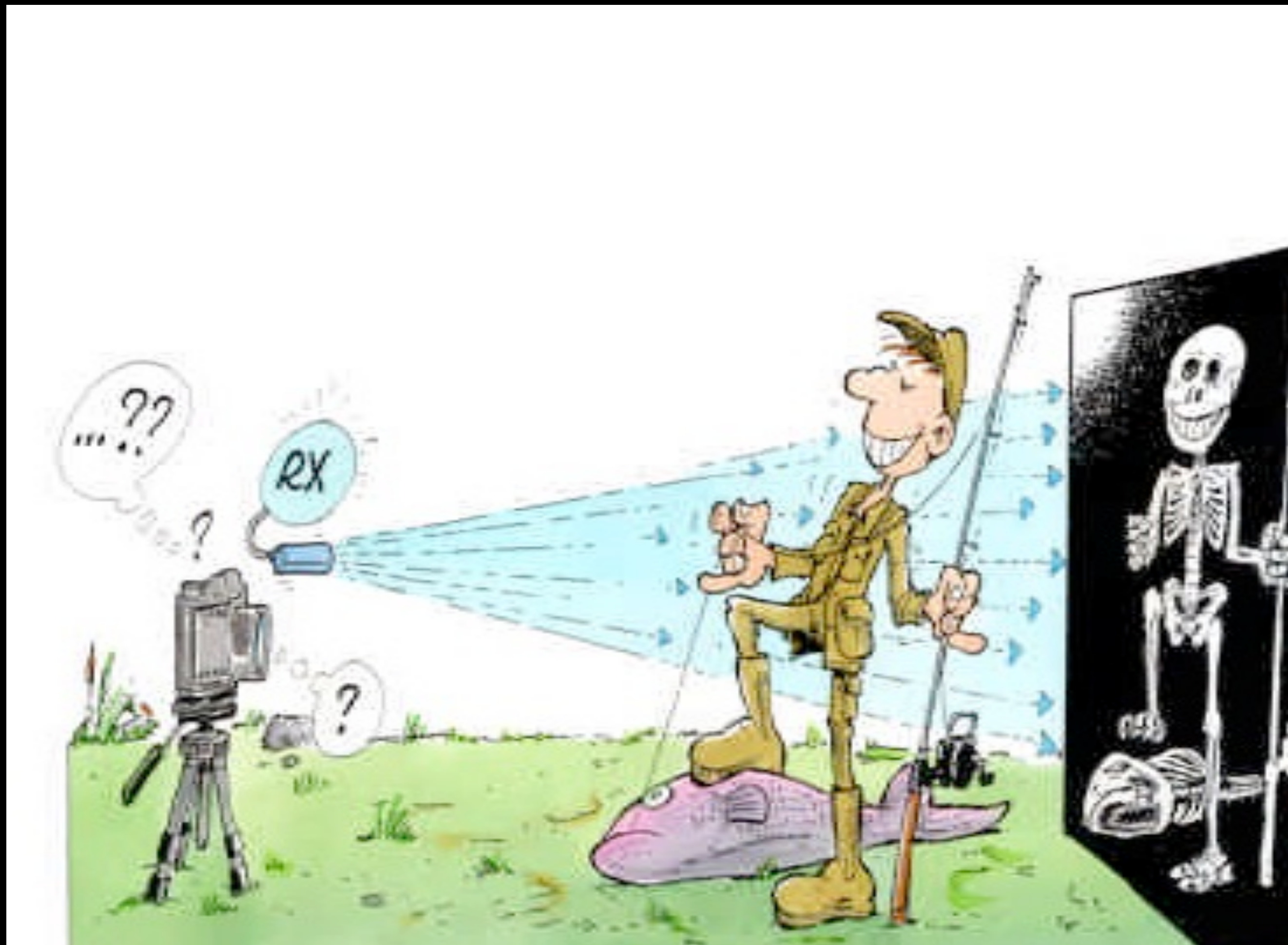

X-ray energy of the most common medical and biological applications

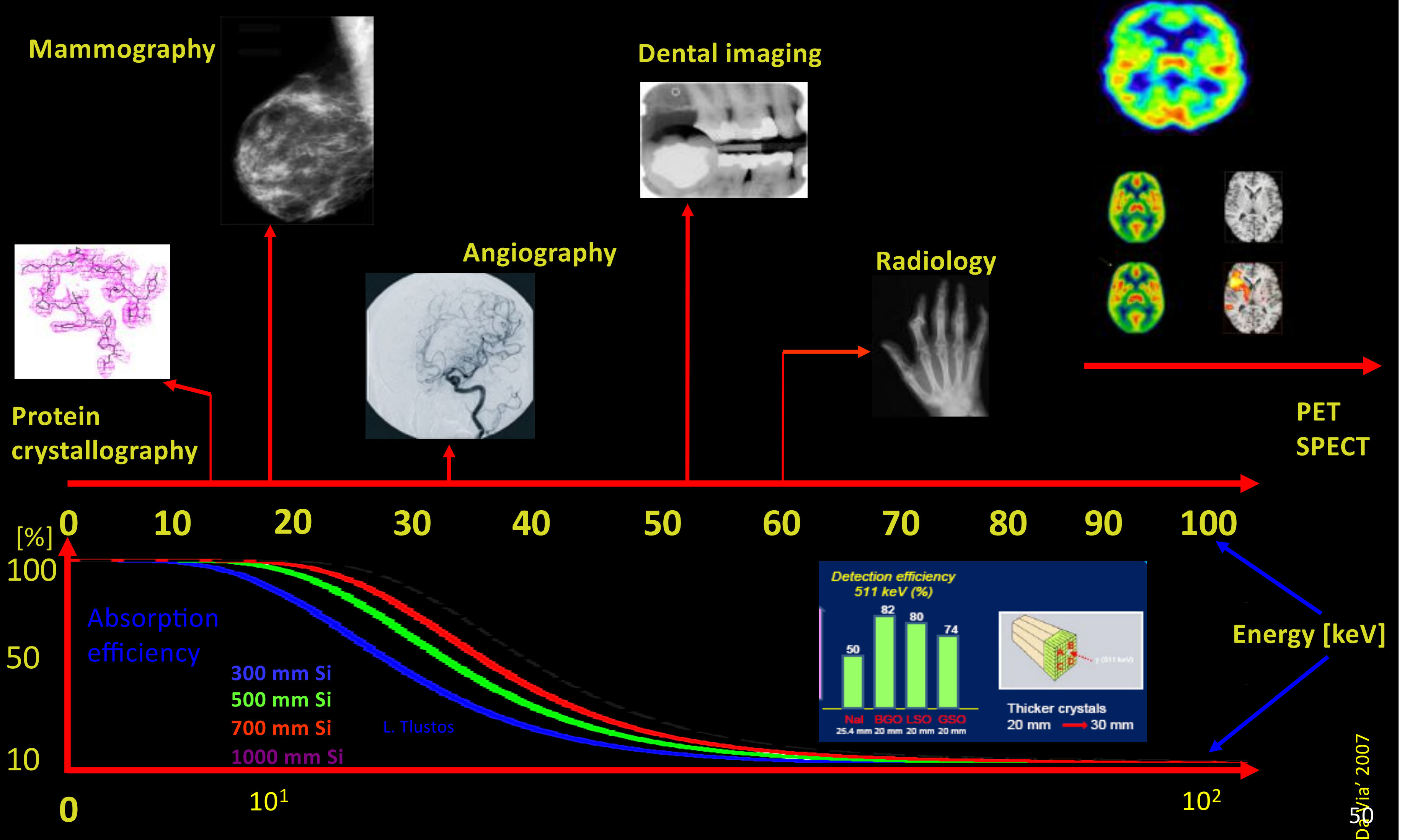

Cinzia Da Via, Uni. Manchester IEEE NPSS Workshop on Applications of Radiation Instrumentation, 2020

Direct / indirect conversion

The target is to reduce the dose to the patient!

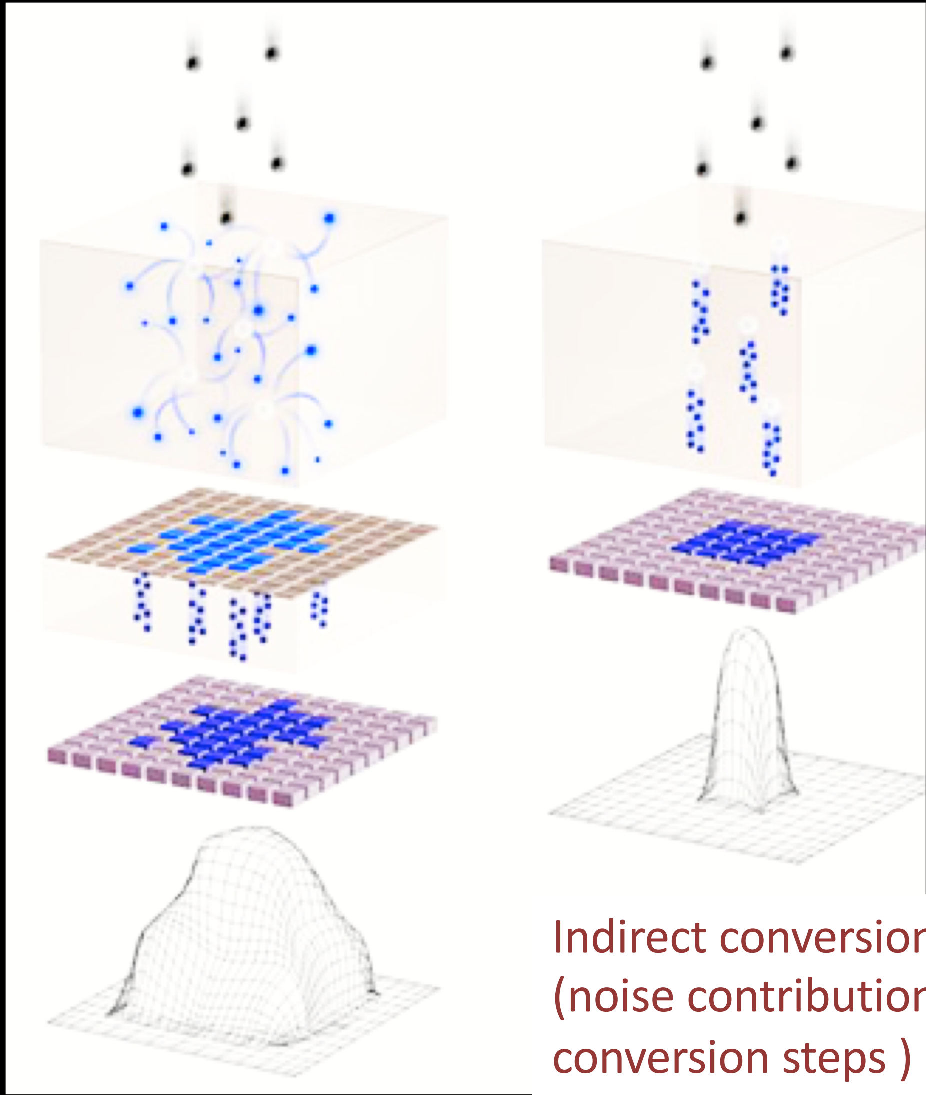

X-rays

Scintillator
Gadox, YAG CsI
(high Z)

Photodiode/ CCD

electronics

electronics

Sampled image

Direct conversion
Si, Ge, CdTe,
GaAs, Se

Sampled image

Indirect conversion implies lower DQE (noise contribution from the two conversion steps)

High Z semiconductors: CdTe and CdZnTe

Taka Tanaka (SLAC/KIPAC)

- High detection efficiency
- Poly-crystalline material
- Poor uniformity
- Very high resistivity (semi-insulating)
- Low leakage current

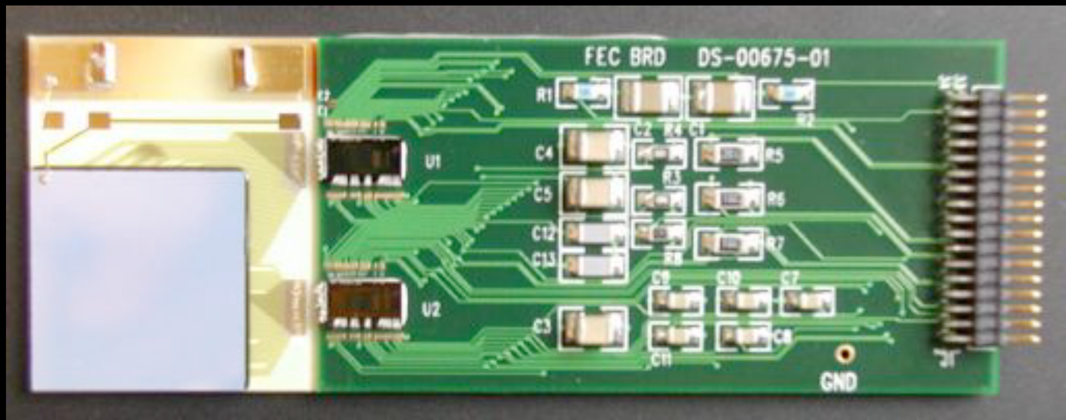

area: 18 " 18 mm2
thickness: 0.5 mm
pixel size: 2 " 2 mm2,
64 ch, cathode side
guard ring: 1 mm width

Fabricated at IDEAS Norway

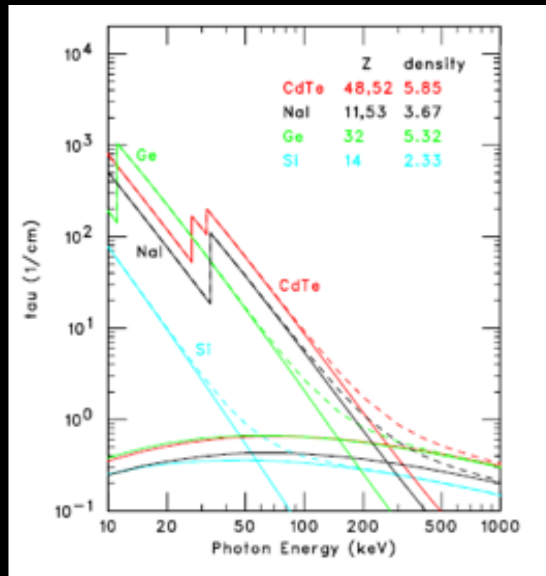

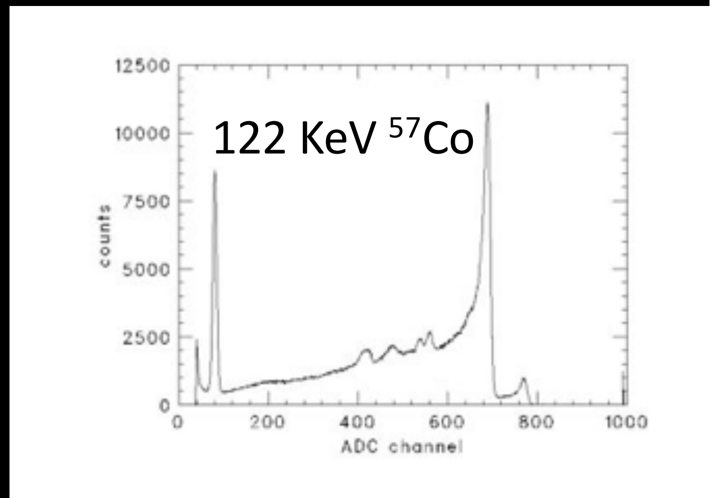

Cinzia Da Via, Uni. Manchester IEEE NPSS Workshop on Applications of Radiation Instrumentation, 2020

MANCHESTER 1824

Indirect Conversion: Scintillators and Silicon Photomultipliers (SiPm, GM-APD, MPPC…)

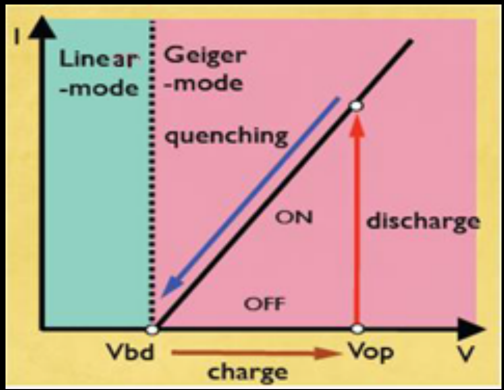

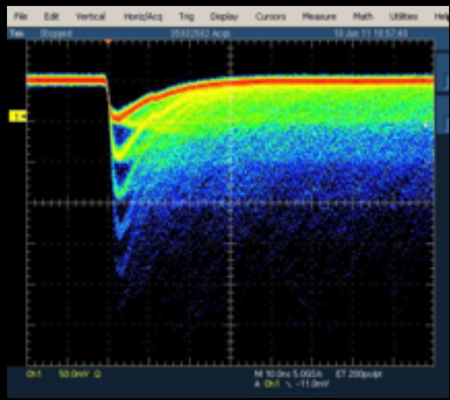

1 pixel
2 pixels
3 pixels

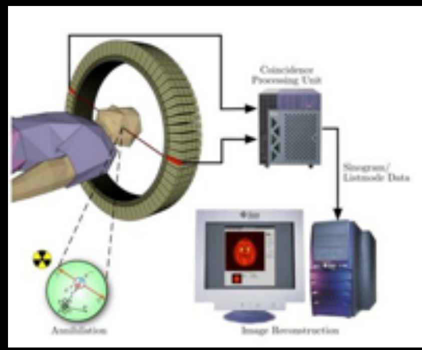

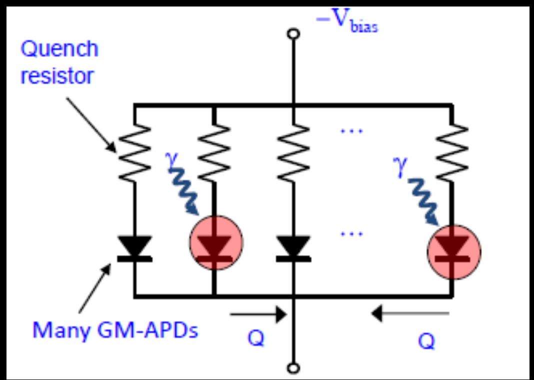

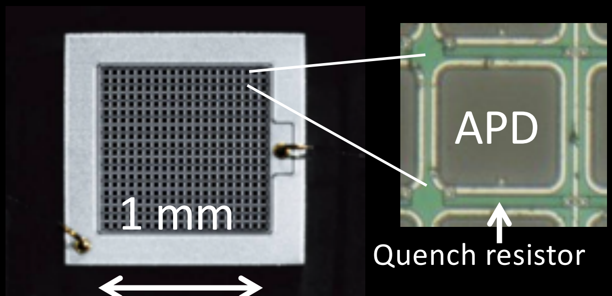

Quench resistor

- SiPm requires a special doping profile to allow a high internal field (>10^5 V/cm) which generates avalanche multiplication
- APD cell operates in Geiger mode (= full discharge), however with (passive/active) **quenching**.
- The avalanche formation is intrinsically very fast (100ps), because confined to a small space.
- High Gain G ~ 10^5 -10^6 at rel. low bias voltage (<100 V)
- G is Sensitive to temperature and voltage variations
- Fill factor still low due to quench resistor on the surface (but work in progress to solve this)

Applications in PET

coincidence of two 511 keV photons define a line of record.

•Take projections under all angles

•(2/3D) Tomographic reconstruct of data

SiPm Commercial Activity

From C. Joram CERN

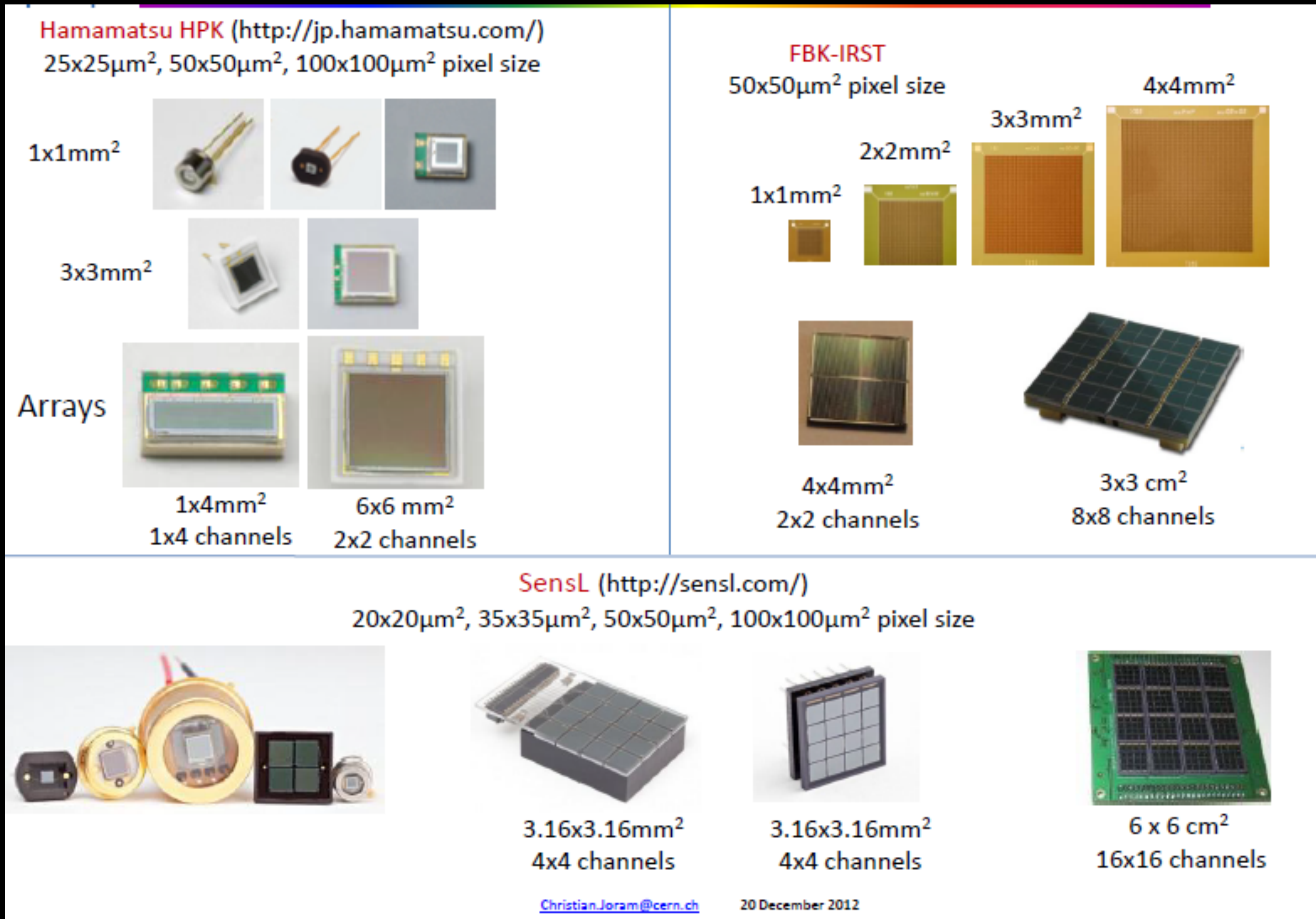

Applications: Protein crystallography

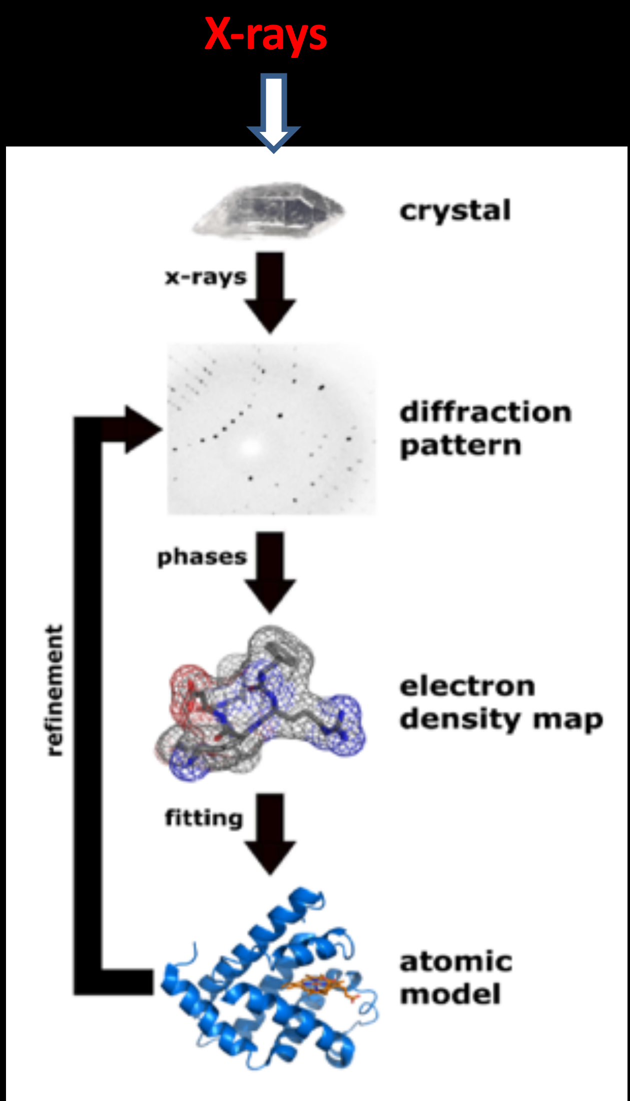

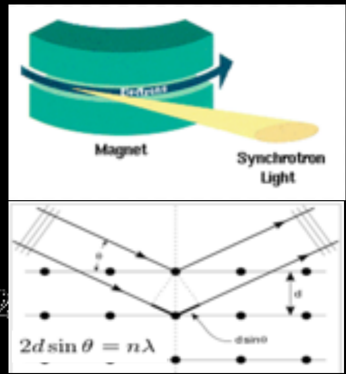

Bragg Law

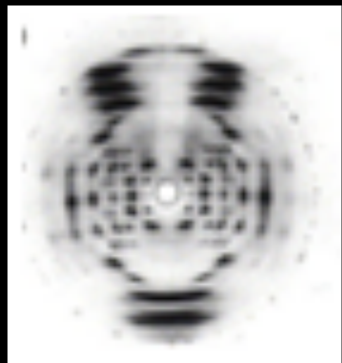

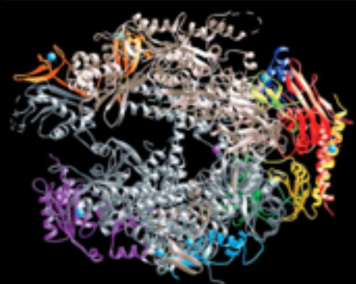

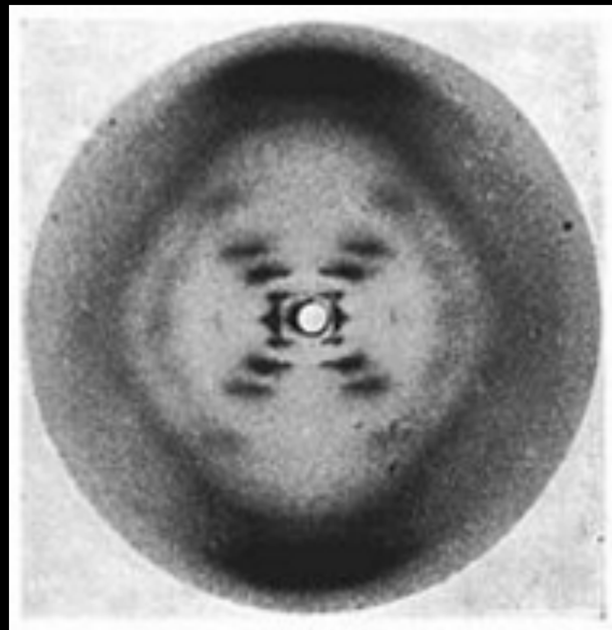

X-ray diffracted Photographic image of the double helix taken in 1952 by Rosalind Franklin and Raymond Gosling. The DNA sample was fibrous DNA

Some of the existing electronics chips

Single photon Counting — Charge Integration

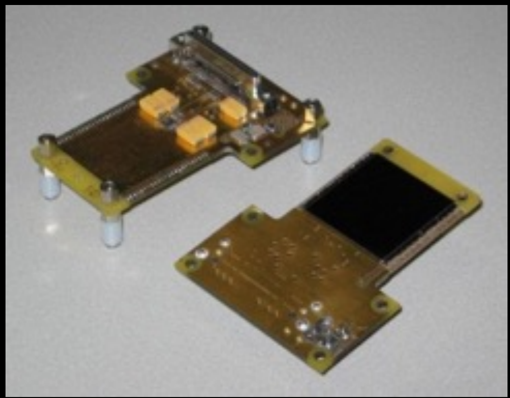

Medipix

pixellated detector
(Si, GaAs, CdTe, 3D
thickness:
300/700/1000mm

MORE ON THIS!

Medipix2 Quad
Pixels: 512 x 512
Pixel size: 55 x 55 mm^2
Area: 3 x 3 cm^2

Gotthard

AGIPD

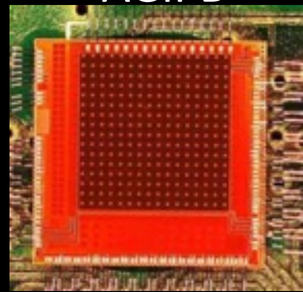

Mithen II

Eiger

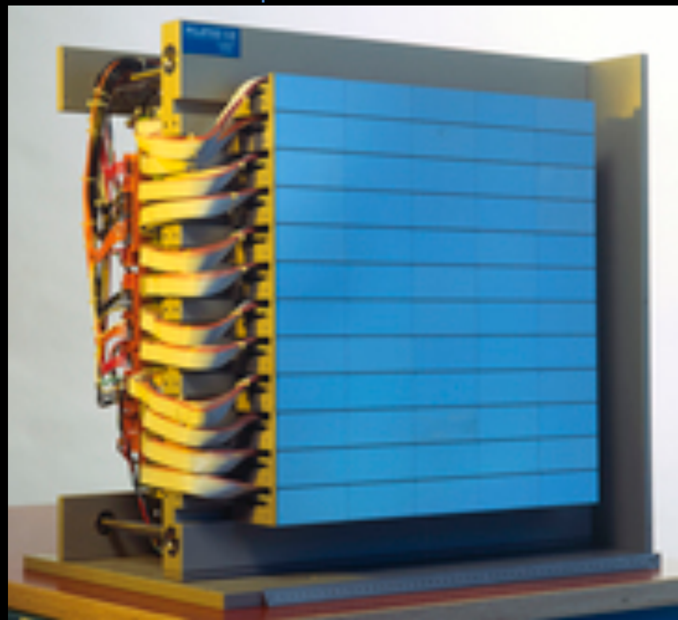

The PILATUS 6M,

424 x 435 mm2 with 170 × 170 μm^2 (2463 x 2527) 6 million pixels, has been developed at PSI and commercialized by the company Dectris for synchrotron imaging

Conclusions and Reflections

We had a look at some properties and parameters of strips and pixel detectors and their evolution since their first use in scientific applications (a lot is missing..)

I would encourage you to meditate on:

- How the signal is formed and detected
- How a detector design develops depending on applications and constraints
- On the past ideas looking towards the future challenges
- On the new ideas (including your own) which might look crazy now but might reveal a true innovation in few years time
- Don't be scared to be different!!!!

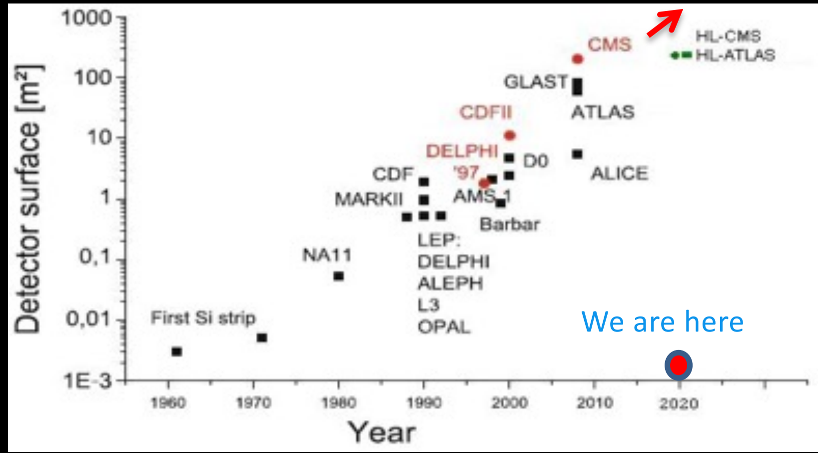

Books on silicon detectors

- Rossi, Fisher, Rohe and Wermes. Pixel Detectors from fundamentals to applications. Springer
- Helmut Spieler. Semiconductor detector systems. OUP Oxford
- Gerard Lutz. Semiconductor Radiation Detectors. Springer
- W. R. Leo. Techniques for Nuclear and Particle Physics Experiments. Springer-Verlag
- C. DaVia, GF. Dalla Betta, S. Parker, Radiation Sensors with 3D electrodes, CRC Press

Thanks to:

Daniela Bortoletto, CERN Summer Student Lectures
Patrick Le Du, EDIT School
Helmut Spieler, Lecture notes (IBL)
Hartmut Sadrozinski, GianLuigi Casse,
Michael Moll, PhD Thesis
Steve Watts, CERN Academic Training
Harris Kagan,
Roland Horisberger,
Marco Povoli, PhD thesis
Gregor Kramberger
Andrea Castoldi,
Chris Damerell,
Sherwood Parker,
Erik Heijne,
Ariella Cattai
Giulio Pellegrini
GianFranco Dalla Betta
Adriano Lai